Lehigh University
Lehigh Preserve

Theses and Dissertations

2002

Ammonia removal from fly ash using a continuously operating acoustically assisted fluidized bed

Kenneth Bradford Lawton
Lehigh University

Follow this and additional works at: http://preserve.lehigh.edu/etd

Recommended Citation
Lawton, Kenneth Bradford, "Ammonia removal from fly ash using a continuously operating acoustically assisted fluidized bed" (2002). *Theses and Dissertations.* Paper 733.

This Thesis is brought to you for free and open access by Lehigh Preserve. It has been accepted for inclusion in Theses and Dissertations by an authorized administrator of Lehigh Preserve. For more information, please contact preserve@lehigh.edu.

Lawton, Kenneth Bradford

Ammonia Removal from Fly Ash Using a Continuously Operating Acoustically…

June 2002

AMMONIA REMOVAL FROM FLY ASH USING A CONTINUOUSLY OPERATING ACOUSTICALLY ASSISTED FLUIDIZED BED

by

Kenneth Bradford Lawton

A Thesis

Presented to the Graduate Committee

of Lehigh University

in Candidacy for the Degree of

Master of Science

in

Mechanical Engineering

Lehigh University

March, 2002

CERTIFICATE OF APPROVAL

This thesis is accepted and approved in partial fulfillment of the requirements for the degree of Master of Science.

Date: 3/28/02

Thesis Advisor: _____

Dr. Edward K. Levy

Chairman of Department: _____

Dr. Charles R. Smith

ACKNOWLEDGMENTS

I would like to thank my family for their support and encouragement throughout this endeavor and every other endeavor that I have undertaken. I would also like to thank my advisor Dr. Edward K. Levy for his guidance and support throughout my work.

The work in this thesis was made possible by funding from The Department of Energy, US Genco, Constellation Energy, PSEG, Ontario Power Generation, Inc., PPL, Inc., Cinergy Corporation and First Energy Corporation. Their support of this project is greatly appreciated.

Finally, I would like to thank DeShau Huang, Matthew Dubrovich, Gerald Trumbauer, Jodi Johnson, and Tamra Lee for their time and assistance. I would also like to thank all of my friends for their encouragement.

TABLE OF CONTENTS

	Page
TITLE PAGE	
CERTIFICATE OF APPROVAL	ii
ACKNOWLEDGMENTS	iii
TABLE OF CONTENTS	iv
LIST OF TABLES	vi
LIST OF FIGURES	vii
ABSTRACT	1
1. INTRODUCTION	2
2. DESIGN EXPERIMENTS	7
Measuring Heat Transfer Coefficient	7
Heater Arrangement	11
Bed Depth and Sound Pressure Level Testing	15
Selecting a Distributor Material	22
3. DESIGN ANALYSIS	25
The Plenum Section	25
The Heated Section	26
Power Requirements	26
The Cooled Sections - Heat Exchanger Analysis	28
Height of the Bed	32
Instrumentation	34

	Page
4. SYSTEM OPERATION	39
Initial Testing and Modifications	39
Measurement of Sound Pressure Levels	42
Measurement of Ash Temperatures	45
Tests with Nanticoke Ash	55
Ash Properties	55
Ammonia Removal in the Batch Bed	58
Ammonia Removal in the Continuous Bed	60
5. ENERGY BALANCE	67
Screw Feeder Calibration	67
Heat Loss Calculations	68
CONCLUSIONS AND RECOMMENDATIONS	73
REFERENCES	74
VITA	75

LIST OF TABLES

		Page
Table 3.1:	Summary of the Dimensions and Process Conditions for the New Bed	36
Table 4.1:	Physical Properties of the Nanticoke Ash	58
Table 5.1:	Calibration of the Screw Feeder	67
Table 5.2:	Summary of Conditions and Assumptions Made in the Energy Balance	71
Table 5.3:	Summary of the Results of the Energy Balance	72

LIST OF FIGURES

		Page
Figure 1.1:	Sketch of Proposed Fluidized Bed	6
Figure 2.1:	Inclined Fluidized Bed Setup with a Single Heater	8
Figure 2.2:	Thermocouple Arrangement to Measure Heat Transfer Coefficients	10
Figure 2.3:	Average Heat Transfer Coefficients for a Single Heater	11
Figure 2.4:	Simulated Heater Bundle in an Inclined Fluidized Bed	12
Figure 2.5:	Average Heat Transfer Coefficients for a Bundle with 4.45 cm Spacing	13
Figure 2.6:	Heat Transfer Coefficients for 4.45 cm Spacing vs Mass Flow Rate	14
Figure 2.7:	Heat Transfer Coefficients for All Three Arrangements	15
Figure 2.8:	15.24 cm Cylindrical Batch Bed Setup	16
Figure 2.9:	Standing Waves for a 5-cm Deep Bed	18
Figure 2.10:	Standing Waves for a 9-cm Deep Bed	18
Figure 2.11:	Standing Waves for a 13-cm Deep Bed	19
Figure 2.12:	Standing Waves for a 15-cm Deep Bed	19
Figure 2.13:	Standing Waves for a 20-cm Deep Bed	20
Figure 2.14:	Standing Waves for a 25-cm Deep Bed	20
Figure 2.15:	Standing Waves for All Tested Bed Depths at 80 Hz	22
Figure 2.16:	Cylindrical Batch Bed Setup With a Layer of Sand or Steel Beads	23

Page

Figure 2.17: Standing Waves in a 13-cm Deep Bed with and without a 1.5-cm Layer of Sand 24

Figure 3.1: Drawing of the Plenum Section 26

Figure 3.2: Surface Temperature of the Heaters vs the Number of Heaters. 28

Figure 3.3: The Number of Tubes Necessary to Sufficiently Cool the Ash 32

Figure 3.4: Cartridge Heater that was Used in the Fluidized Bed 33

Figure 3.5a: CAD Drawing of the Heated and Entrance Sections 37

Figure 3.5b: CAD Drawing of the Cooled Sections 38

Figure 4.1: Sketch of Modifications made to the Plenum Section 41

Figure 4.2 Experimental Setup for SPL Measurements 43

Figure 4.3: Waveforms Observed in the Heated Section 44

Figure 4.4 Sound Pressure Levels for the Entire Heated Section 45

Figure 4.5: Thermocouple Setup in the New Fluidized Bed 47

Figure 4.6: Fly Ash Temperatures in the Heated and Cooled Sections 48

Figure 4.7: Fly Ash Temperature in the Heated and Cooled Sections with 7 Additional Heaters 49

Figure 4.8: Equilibrium Temperature Distribution for the Entire Bed 50

Figure 4.9: Ash Temperatures in the Heated Section with a Flow Rate of 75.3 kg/hr 51

Page

Figure 4.10: Ash Temperatures in the Heated Section with a Flow Rate of 101.2 kg/hr 52

Figure 4.11: Ash Temperatures in the Heated Section with a Flow Rate of 113.4 kg/hr 52

Figure 4.12: Mass Flow Rate Measurements 53

Figure 4.13: Ash Temperature in the Heated Section for Changes in Flow Rate 54

Figure 4.14: Ammonia Concentration of the Ash in the Batch Bed 54

Figure 4.15: Ammonia Concentration as a Percent of the Original Concentration 60

Figure 4.16: Fly Ash Temperature and Mass Flow Rate for the Entire Test 62

Figure 4.17: Ammonia Concentration and Ash Temperature for the Entire Test 63

Figure 4.18: Ammonia Concentration and Mass Flow Rate for the Entire Test 64

Figure 4.19: Ammonia Concentrations for Tests in the Batch Bed and the Continuously Operating Bed 65

Figure 4.20: LOI and Mean Particle Size of the Processed Ash 66

Figure 5.1: Diagram for Radiation Calculations 68

Figure 5.2: Calculated Sidewall Temperature Distribution 69

ABSTRACT

The Environmental Protection Agency (EPA) has set strict limits on the amount of Nitrogen Oxide (NO_x) that a power plant can emit. To lower the NO_x emissions, most coal fired power plants use selective or non-selective catalytic reduction. During this process ammonia is injected into the boiler. This ammonia reacts with the NO_x to form nitrogen and water. Invariably, some of the ammonia is adsorbed by the fly ash in the stack. This contaminated fly ash is then unsuitable for utilization. Many applications such as mixing concrete and mine reclamation utilize uncontaminated fly ash.

Laboratory tests have shown that heating the fly ash to a sufficiently high temperature in a fluidized bed, operating in the batch mode, reduces the ammonia concentration to acceptable levels. A continuously operating fluidized bed for the removal of ammonia from fly ash has been designed, built, and tested. Larger than expected energy losses led to a lower than desired mass flow rate of ash. The experiments presented in this thesis show that more than 95 percent of the ammonia could be driven off, during continuous operation, when the temperatures are above 385 C. Therefore, the continuously operating acoustically assisted fluidized bed is an effective way of removing ammonia from fly ash.

CHAPTER 1: INTRODUCTION

In 1999, coal-fired power plants provided 56 percent of the power generation in the United States [1]. Steel production in the United States also relies heavily on coal fired blast furnaces. Many other commercial and residential applications use coal as an energy source. Coal is inexpensive compared to other fossil fuels and experts estimate that at current usage levels the coal reserves of the world will last more than 200 years [1]. More importantly, the United States has vast coal reserves, some of which are still undiscovered. Unlike other power sources the waste product associated with coal combustion, fly ash, can be utilized in a variety of ways.

In 1996, 27.4% of the fly ash produced in the United States was utilized in one form or another. The remaining ash was discarded to landfills. Fly ash is currently used as an addition to cement and concrete, structural fill and cover material, waste stabilization/solidification, roadway and pavement utilization, an addition to construction materials as a light weight aggregate, infiltration barrier and underground void filling, and soil, water and environmental improvement. Approximately 70% of the ash produced within the Commonwealth of Pennsylvania is used as a means of restoring its 225,000 acres of abandoned mine-lands [2]. The largest national use for fly ash is as an additive to concrete. Adding fly ash to cement benefits the mixing and structural properties of the concrete. The use of fly ash in cement reduces the water to cement ratio. Due to

the fact that the ash particles are smaller than that of the aggregate, the amount of air entrained in the concrete is dramatically lower [2]. If fly ash is used, less Portland cement material is needed, therefore project costs are lowered. Finally, the addition of fly ash to the concrete, if used in the correct proportions causes the concrete to have a greater overall strength than concrete with Portland cement alone[2].

One major problem in the combustion of coal is the amount of nitrogen oxide (NO_x) released to the environment. NO_X is the main cause of acid rain. The Environmental Protection Agency has placed strict limits on the amount of NO_X that can be released and future regulations further lower the allowable limits. One solution to the NO_X problem has been to use selective catalytic reduction (SCR) and non selective catalytic reduction (NSCR). In these processes ammonia is injected into the flue gas, where it reacts with the NO_X to produce nitrogen and water. Some of the ammonia in the flue gas gets adsorbed by the fly ash. The ammonia in the fly ash presents several problems with the utilization and land filling of the fly ash.

Any utilization of ammonia contaminated fly ash, where the ash comes in contact with moisture, presents the possibility of contamination. The moisture causes the ammonia to desorb from the fly ash. Ammonia that desorbs into the air or ground water leads to two potential problems. The ammonia in air concentrations at landfills, around processing equipment, or the use of the

ammoniated fly ash in commercial products, can lead to hazardous concentrations or at least concentrations objectionable to operating personnel. The use of ammoniated ash in concrete is of more concern since the largest amount of ash is used in this application. The odor problems that arise while mixing and pouring make the use of ammoniated ash unacceptable in this venue. Brugghen showed that the compressive strength of concrete is dramatically lowered when fly ash with high levels of ammonia is used [3].

There is a need for a process to be developed that removes all or an acceptable level of the ammonia from the contaminated ash so that it can be utilized or land filled without causing groundwater, soil, or air contamination. As long as the level of ammonia contamination is kept below 100 ppm, the ammonia can no longer be observed by the olfactory sense and the other applications that use fly ash will not be affected. In laboratory tests using a fluidized bed operating in a batch mode, show that heating the contaminated ash to 399 C reduces the ammonia to acceptable levels [4].

This project involved the development of a continuously operating fluidized bed for the removal of fly ash. The type of bed used in the design of the laboratory model will be a long, narrow, horizontal bed. Ash will enter one end of the bed at a rate of 226.8 kg/hr, be fluidized by air and flow horizontally along the bed. The ash will be heated from room temperature to 399 C and then be cooled to 93 C. The ash will then exit the opposite end of the bed and be

collected into buckets. The new fluidized bed will also use an acoustic field to enhance the fluidization characteristics.

Fine powders are very difficult to fluidize and the fly ash used in the experiments described in this thesis all have mean particle diameters of less than 100 μm. The fluidization of these particles is poor due to van der Waals forces. These forces lead to agglomeration and spouting when fluidization is attempted. However, when a low frequency, high intensity acoustic field is applied the fluidization is greatly enhanced. The spouting and channeling no longer occur and active bubbling is possible. The acoustic waves vibrate the fly ash and overcome the inter-particle forces[5]. The SPL should be higher than 110 dB in order to be of any significance [6]. An SPL of 135 or greater results in the best fluidization and bubbling characteristics [5].

In the presence of an acoustic field many researchers have found that the heat transfer coefficient increases. For fly ash with a mean particle size of 32 μm the heat transfer coefficient nearly triples and for fly ash with a mean particle size of 76 μm the heat transfer coefficient is increased slightly [4]. Figure 1.1 depicts what the new fluidized bed will look like.

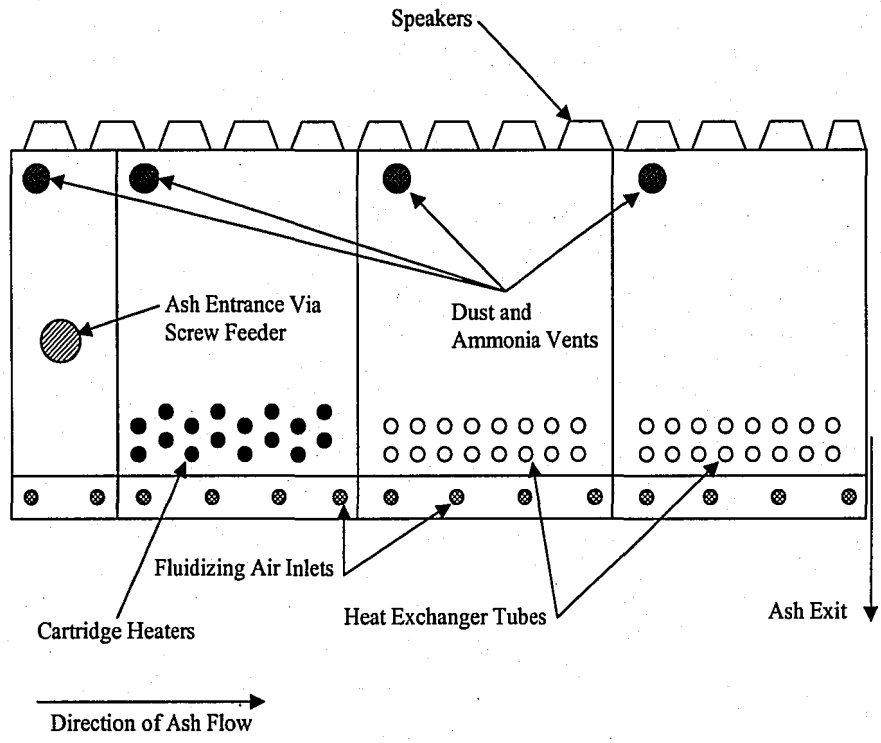

Figure 1.1: Sketch of Proposed Fluidized Bed

CHAPTER 2: DESIGN EXPERIMENTS

To determine various design parameters for the new fluidized bed several experiments were designed and conducted. All of the experiments in this section used fly ash from Homer City unless otherwise noted. This ash, which had been sieved and had the fines removed, had a mean particle diameter of 76 μm. It was thus easy to fluidize without the presence of an acoustic field. In all of the experiments described in this paper the acoustic fields were generated by connecting a BK Precision 3011B 2MHz Function Generator to a Kenwood AM/FM 100-watt Stereo Receiver, model number KR-A5070. The signal generator outputs a square wave and controls the frequency. The speakers used are Radio Shack 8-inch, 100 watt max power, 8 ohm subwoofers. Sound pressure level (SPL) was measured using a microphone connected to a Bruel & Kjaer Type 2609 Measuring Amplifier, 20-20000 Hz. A variable speed screw feeder was used to control the mass flow rate.

Measuring Heat Transfer Coefficient

The purpose of the first experiments was to determine the heat transfer coefficients between the electrical cartridge heaters and the fly ash. For this experiment a fluidized bed, with a nearly horizontal distributor (referred to as an inclined fluidized bed) was used. The bed had an inclination of 2.54 cm in 1.524 m, a width of 10.16 cm and a bed depth of 12.7 cm. For this setup a 500W, 1.27 cm diameter electrical cartridge heater was placed 7 cm above the distributor. A

voltage regulator was connected to the heater to control the heat flux. Figure 2.1 shows how the bed was configured.

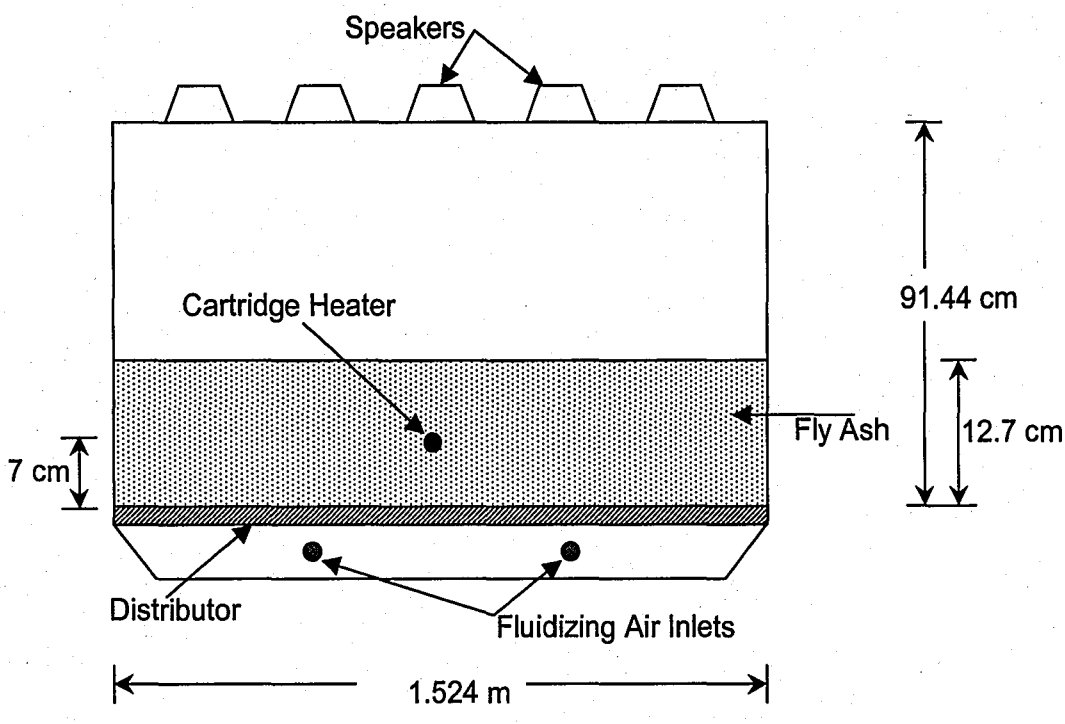

Figure 2.1: Inclined Fluidized Bed Setup with a Single Heater

To find the heat transfer coefficient, equation 2.1 was employed.

$$q = hA(T_{\infty} - T_s) \tag{2.1}$$

where q is the heat transfer rate, h is the heat transfer coefficient, A is the surface area of the heater, T_{∞} is the temperature of the fly ash and T_s is the average surface temperature of the heater. The rate of heat transfer was calculated by finding the power output of the heater. This was done by measuring the Root Mean Square (RMS) voltage applied to the heater and the

resistance of the heater with a multi-meter. Then Equation 2.2 was used to calculate the average power dissipated by the heater.

$$p_{avg} = \frac{V_{RMS}^2}{R} \tag{2.2}$$

where P_{avg} is the average power dissipated, V_{RMS} is the RMS voltage, and R is the resistance of the heater. To measure the fly ash temperature, four thermocouples were located approximately 2.54 cm from the heater. Their measurements were then averaged to determine T_∞. Four thermocouples were attached to the surface of the heater and then averaged to find T_s. The thermocouples were then connected to a Fluke 2175A Digital Thermometer. Figure 2.2 illustrates how the thermocouples were arranged.

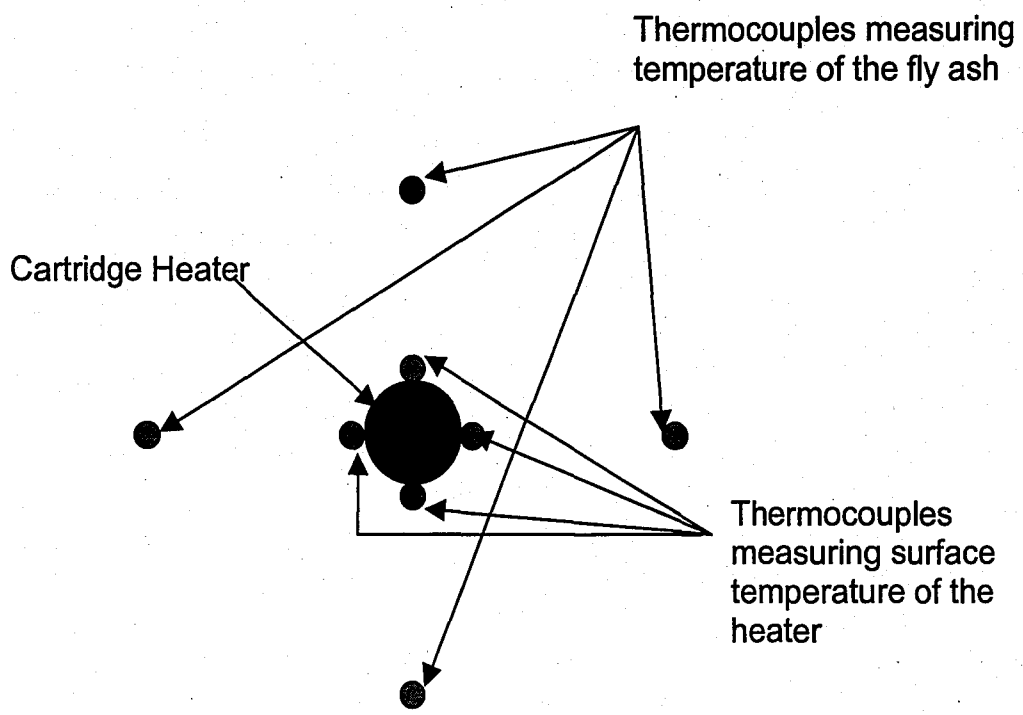

Figure 2.2: Thermocouple Arrangement to Measure Heat Transfer Coefficients

Figure 2.3 shows the results for the heat transfer coefficients for the single heater measured at different mass flow rates. Mass flow rate was calculated by determining the mass of a sample taken for 1 minute at the outlet of the bed. These results show that the heat transfer coefficient was unaffected by changes in mass flow rate. As the air velocity is increased the heat transfer coefficient increases until the bed achieves good bubbling and mixing.

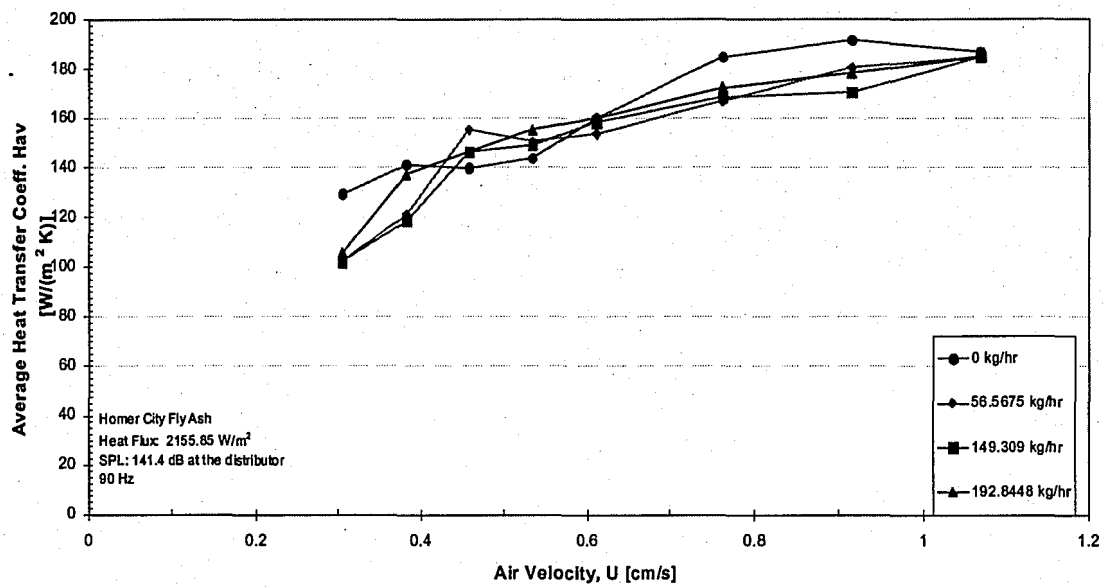

Figure 2.3: Average Heat Transfer Coefficients for a Single Heater

Heater Arrangement

An important design parameter was how to arrange the heaters. Testing was done to determine the minimum distance between the heaters, in order to avoid adversely affecting the heat transfer coefficient. A single heater was placed in the center of a bundle of simulated heaters in order to determine the spacing needed for the design. Wooden dowels of the same diameter as the heater (1.27 cm) were used to simulate other heaters in a staggered array. Figure 2.4 shows how the simulated heater bundle was arranged in the fluidized bed. The thermocouples were arranged in the same manner as shown in Figure 2.2. Three separate tests were run varying the distance d (Figure 2.4). The values

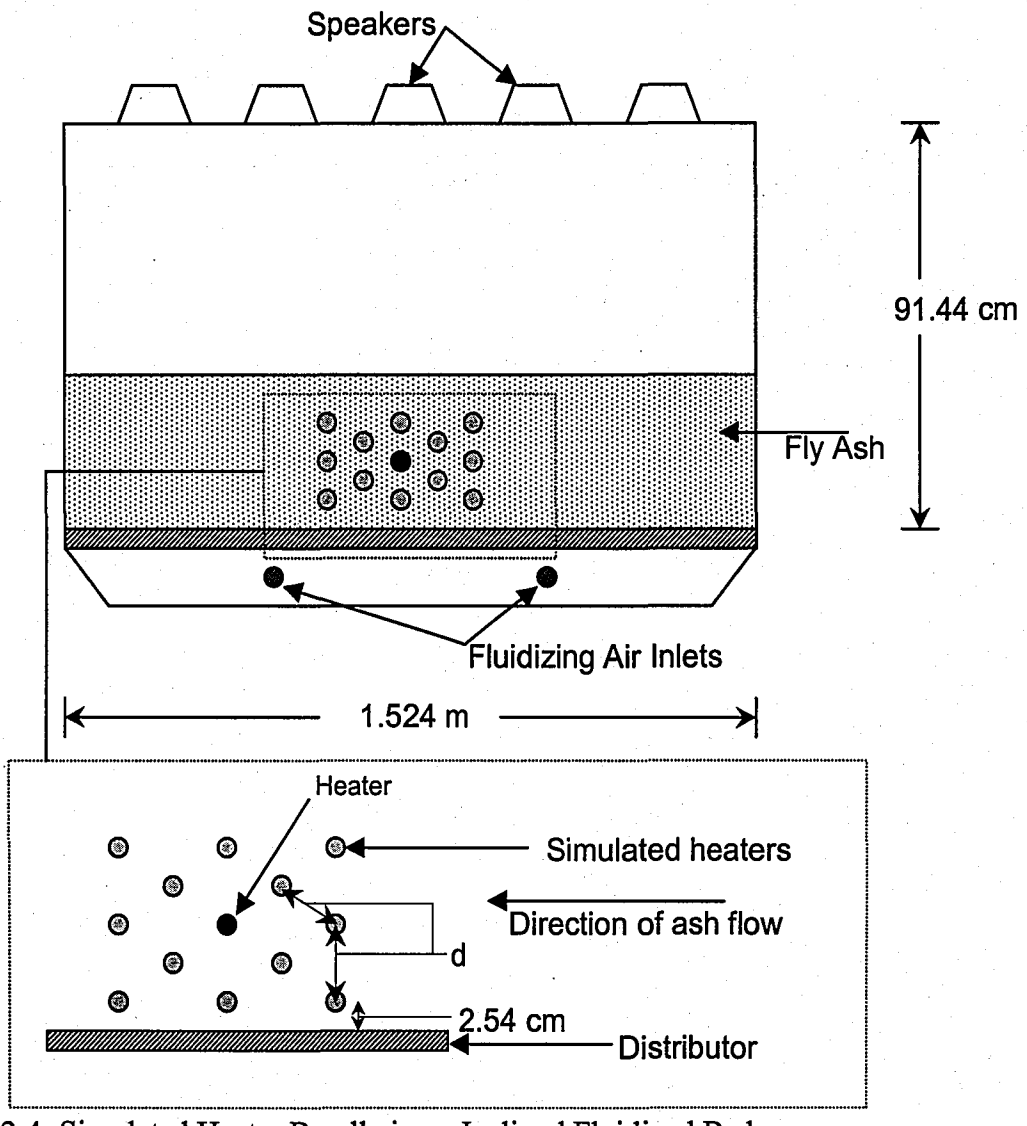

Figure 2.4: Simulated Heater Bundle in an Inclined Fluidized Bed

used were 4.45, 5.1, and 6.35 centimeters. This bundle was then placed in the inclined fluidized bed with an expanded bed depth of 12.7 cm. An acoustic field was supplied at a frequency of 90 Hz. Controlling the speed of the screw feeder, afforded different flow rates of the fly ash. Each spacing was tested at three different flow rates: 0, 104.8, and 193.7 kilograms per hour. For each flow rate

the heat transfer coefficient was measured versus the fluidizing gas velocities. The results for the average heat transfer coefficient for the spacing of 4.45 cm are shown in Figure 2.5. The results of this test show similar results to the single heater test in that mass flow rate has little influence on the heat transfer coefficient and that good fluidization characteristics are important for heat transfer. This test also showed a decrease in the heat transfer coefficients from those in the previous test. One possible explanation of this decrease is that the addition of the bundle caused the flow patterns around the heater to change. Further investigation is needed to explain the results.

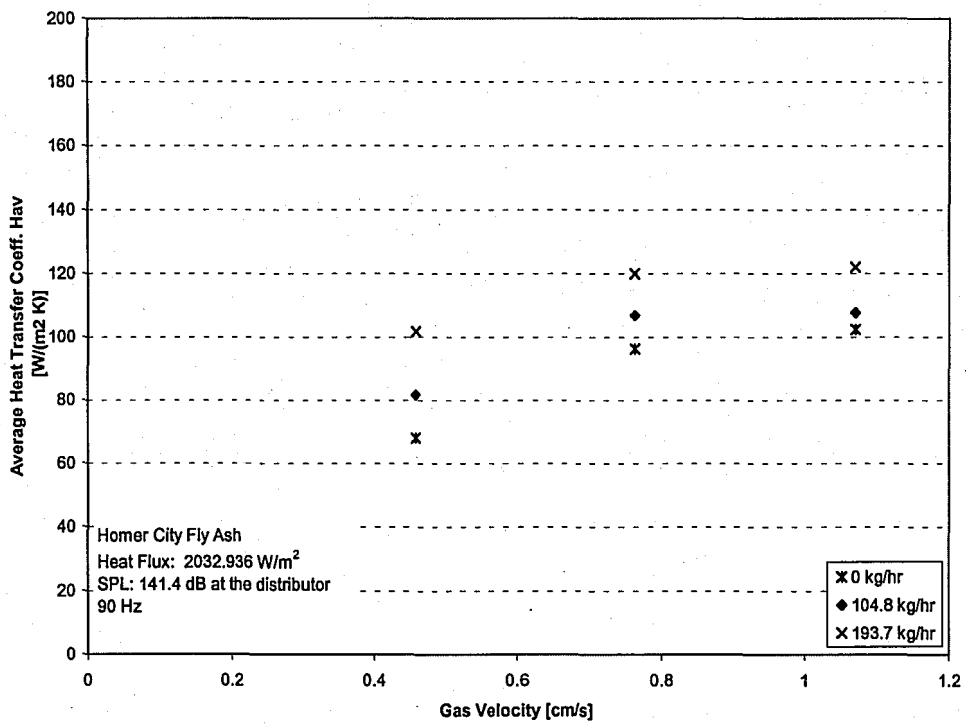

Figure 2.5 Average Heat Transfer Coefficients for a Bundle with 4.45 cm Spacing

Figure 2.6 shows the heat transfer coefficient versus the mass flow rate. Here it is easy to see that heat transfer coefficients change when mass flow is added but that after 100 kg/hr the heat transfer coefficients are relatively unchanged.

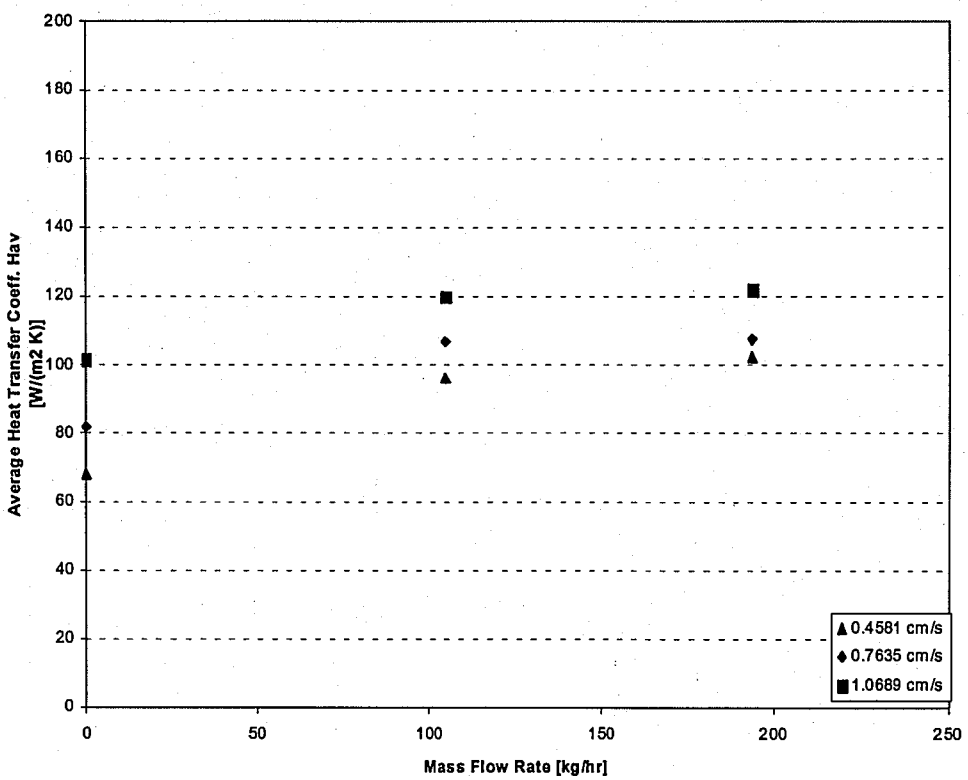

Figure 2.6: Heat Transfer Coefficients for 4.45 cm Spacing vs Mass Flow Rate

The original design specifications define the ideal mass flow rate to be 226.8 kg/hr. Therefore only the results for 193.7 kg/hr will be considered for this design. Figure 2.7 shows these results for all three spacings. It can easily be seen that for the bundle arrangements considered the heat transfer coefficients effectively remain the same. Therefore the heaters will be spaced at 5.1 cm on center in a staggered array for the new design.

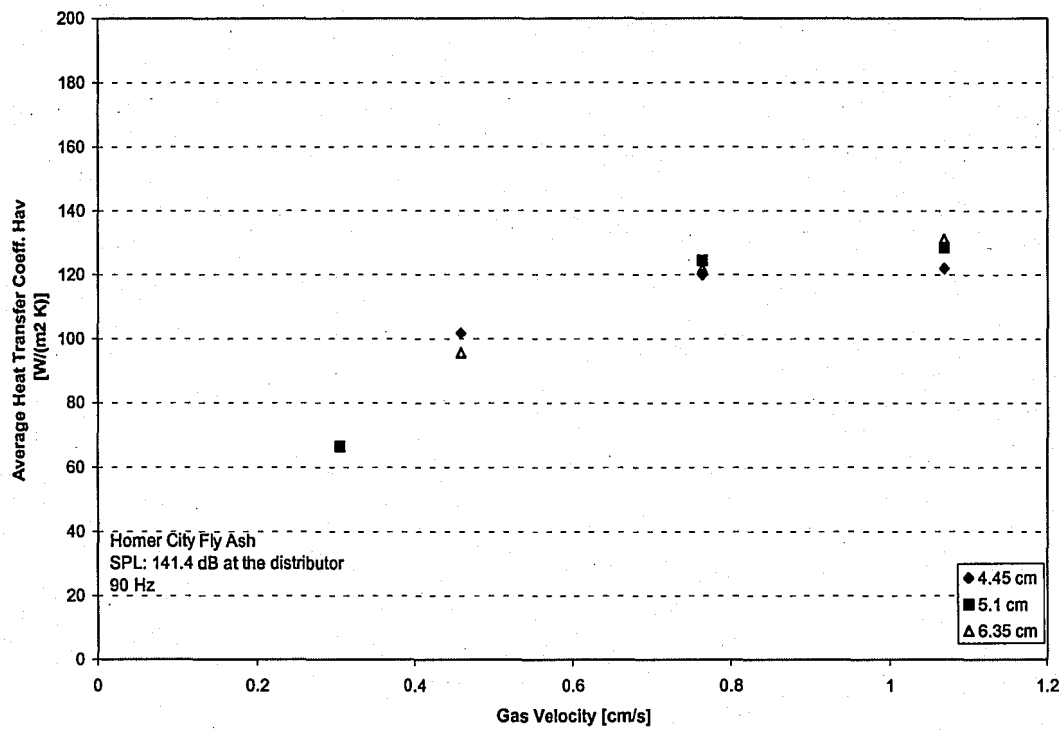

Figure 2.7: Heat Transfer Coefficients for All Three Arrangements

Bed Depth and Sound Pressure Level Testing

Another design parameter to be found is the depth of fly ash that can be processed through the bed. Two factors influence this parameter. First, the bed must have good fluidization characteristics. This means that there must be good bubbling and good mixing in the bed. The second factor is sound pressure level. In order to get the best heat transfer and bubbling characteristics, the sound pressure must be maximized.

Sound pressure levels are generally the best when a resonance condition exists. In that situation there is an increase in sound pressure level from the free

surface to the bottom of the bed. However, when using deep beds the attenuation becomes significantly larger and the equations that predict the resonance conditions are not accurate. In order to find the best conditions a process of trial and error had to be employed. These tests were carried out in a 15.24 cm diameter cylindrical bed as seen in Figure 2.8.

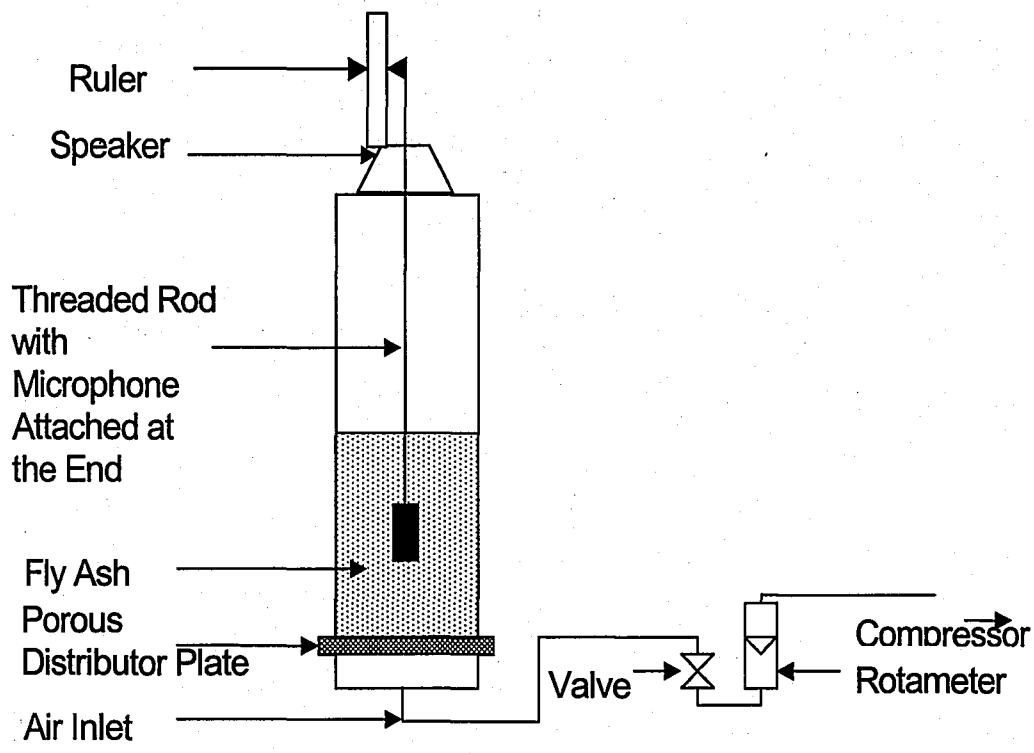

Figure 2.8: 15.24 cm Cylindrical Batch Bed Setup

Tests were conducted on bed depths of 5, 9, 13, 15, 20, and 25 centimeters. For each test the resulting standing waves were recorded for frequencies between 70 and 130 Hz. Higher frequencies were not tested because the attenuation becomes significantly larger as the frequency increases. The distance from the speaker to the free surface, X_R was changed for each

frequency to make that distance a quarter of a wavelength in order to get the maximum SPL at the free surface. To find the distance corresponding to a quarter wavelength, equation 2.3 was used.

$$X_R = \frac{\lambda}{4} = \frac{4c}{f} \tag{2.3}$$

where λ is the wavelength, c is the speed of sound in air, and f is the frequency.

To measure the standing waves in the fluidized bed, the microphone attached to the threaded rod was pulled away from the distributor at 1.27 cm and 2.54 cm intervals. The sound pressure level and the distance from the distributor were then recorded. All tests were performed with a fluidizing air velocity of 0.563 cm/s.

Figures 2.9-2.14 show the standing waves for bed depths of 5, 9, 13, 15, 20, and 25 cm respectively.

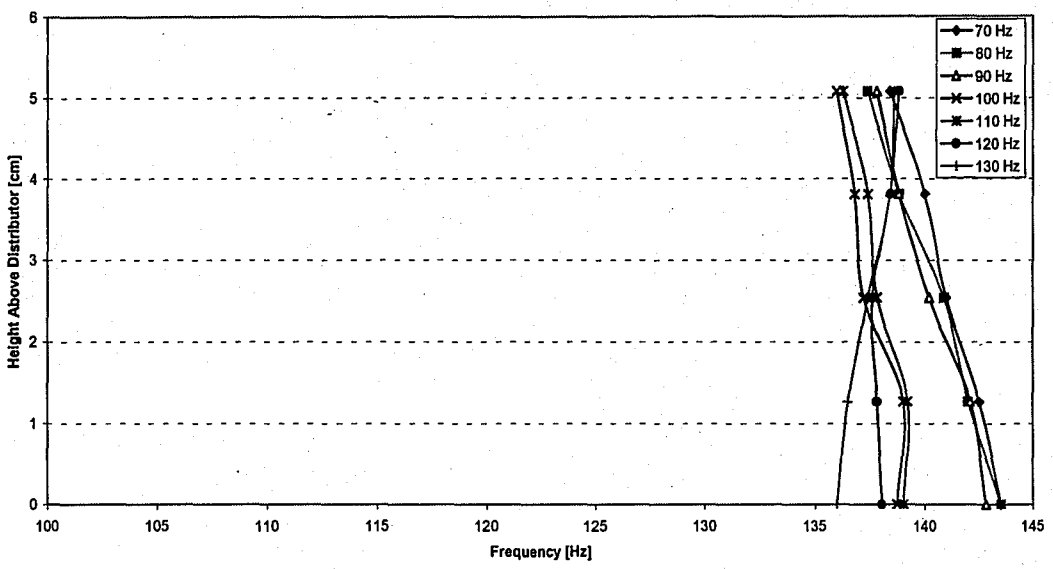

Figure 2.9: Standing Waves for a 5-cm Deep Bed

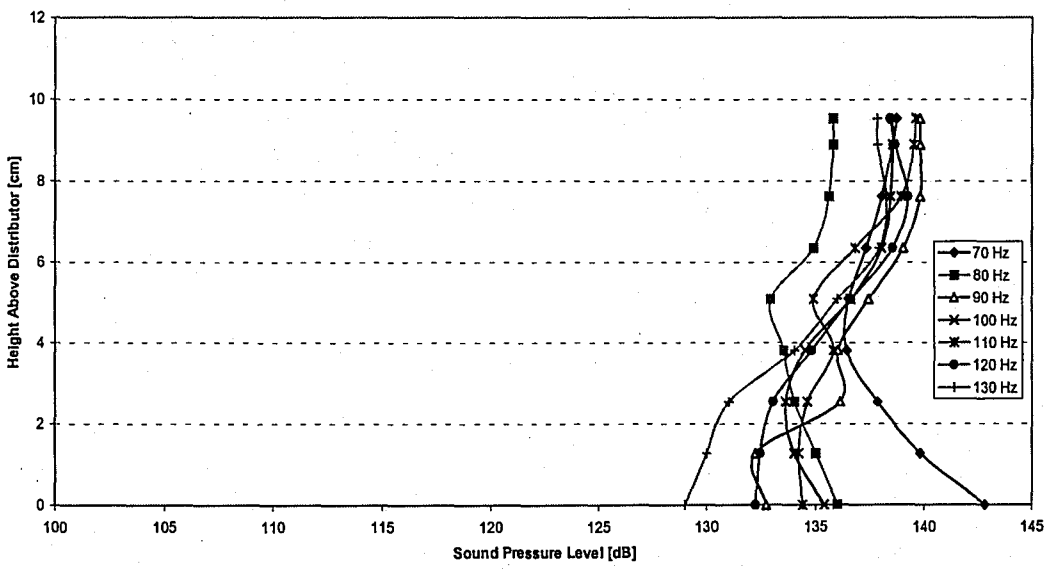

Figure 2.10: Standing Waves for a 9-cm Deep Bed

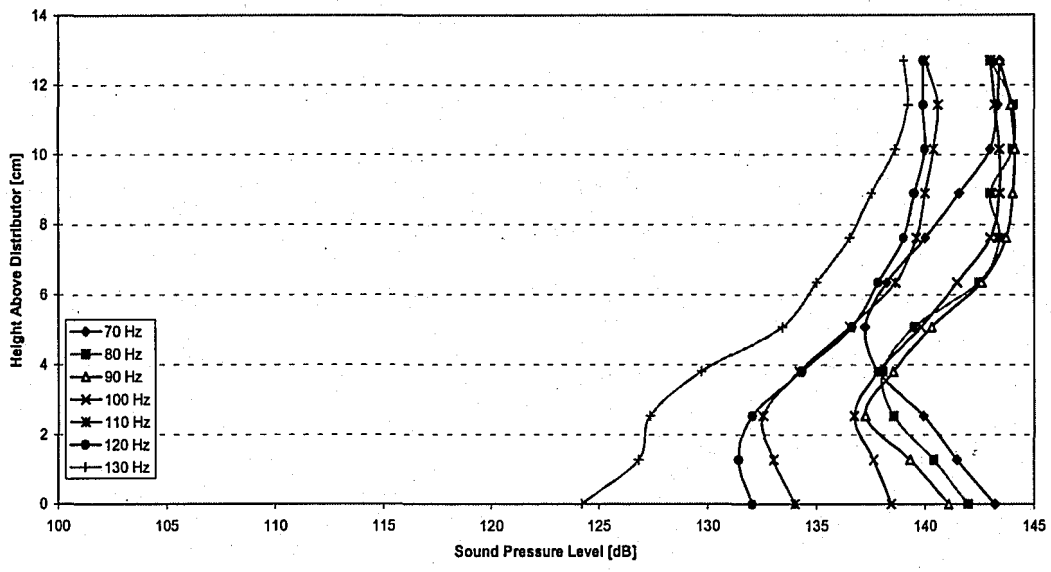

Figure 2.11: Standing Waves for a 13-cm Deep Bed

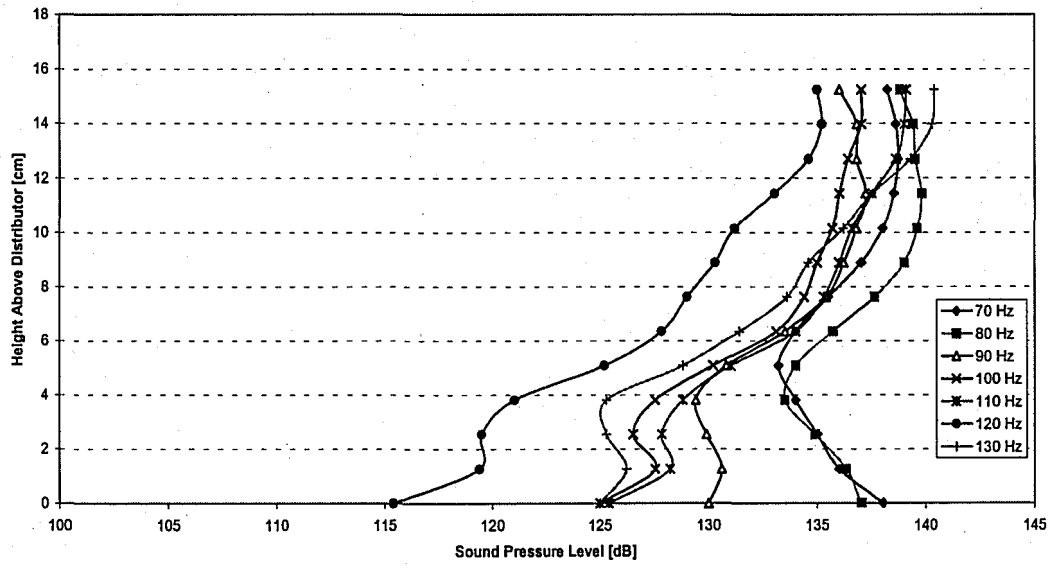

Figure 2.12: Standing Waves for a 15-cm Deep Bed

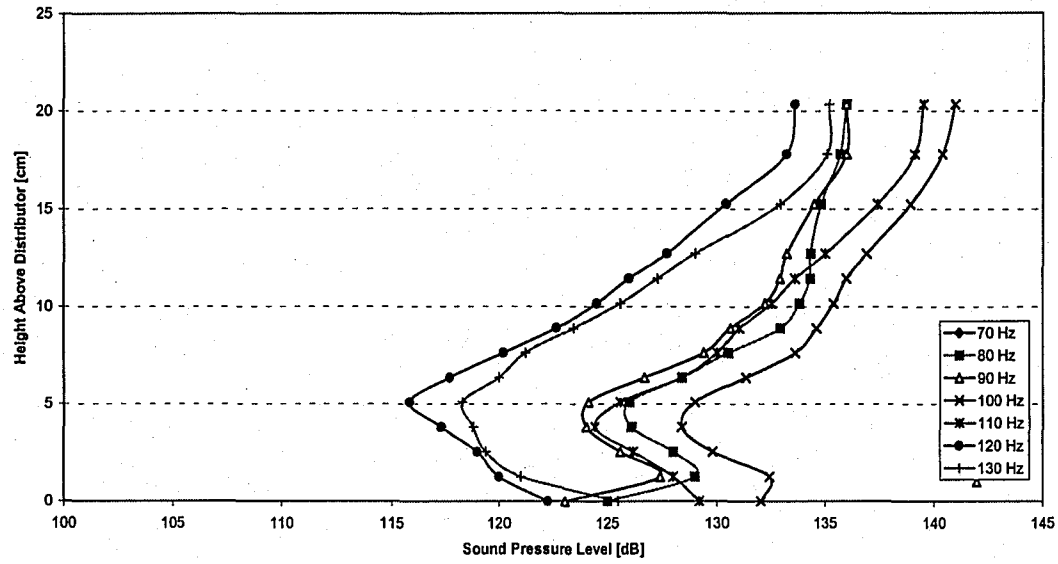

Figure 2.13: Standing Waves for a 20-cm Deep Bed

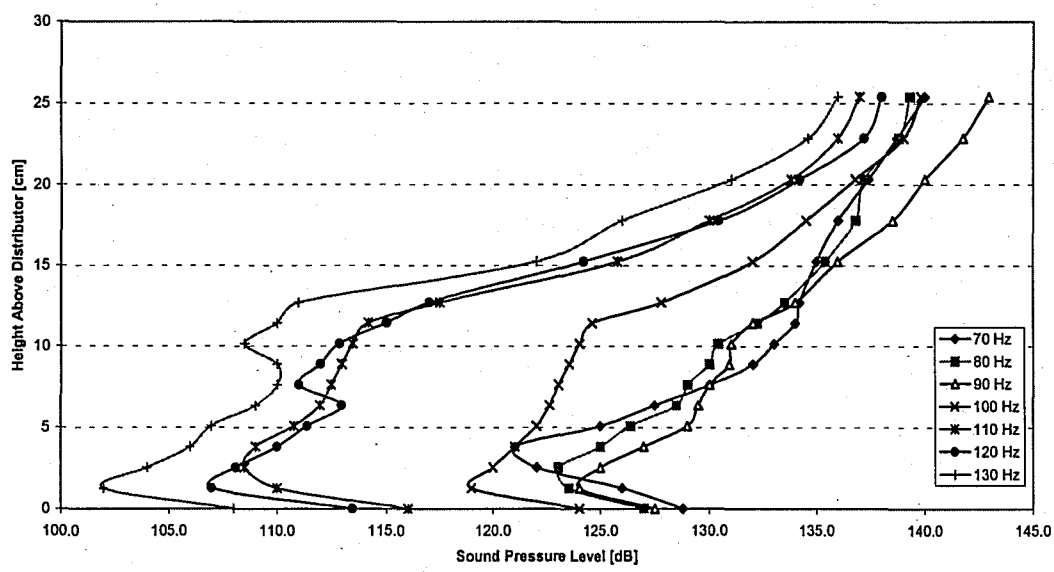

Figure 2.14: Standing Waves for a 25-cm Deep Bed

In the 5 centimeter bed, Figure 2.9, the resonance condition can easily be seen as an increase in sound pressure level from the free surface of the bed to the distributor. Figure 2.10, representing the 9 cm bed shows the effects of attenuation but the sound pressure levels remain high. The deepest bed depth to have relatively low attenuations is the 13 cm bed seen in Figure 2.11. In Figures 2.12, 2.13, and 2.14 the effects of attenuation are obvious. Sound pressure levels decrease from the free surface to the distributor on the order of 10 dB and greater. For all of the depths, a frequency of 80 Hz achieves the best condition. Figure 2.15 shows the standing wave for all of the tested bed depths at a frequency of 80 Hz. The attenuation losses in bed depths of 15, 20, and 25 centimeters are too great for use in this application and a bed depth of 10 or less does not permit enough fly ash to be processed. A bed depth of 13 centimeters however, results in high sound pressure levels and low attenuations while keeping a relatively deep bed. Therefore, the new fluidized bed will operate with a bed depth of 13 centimeters at a frequency of 80 Hz.

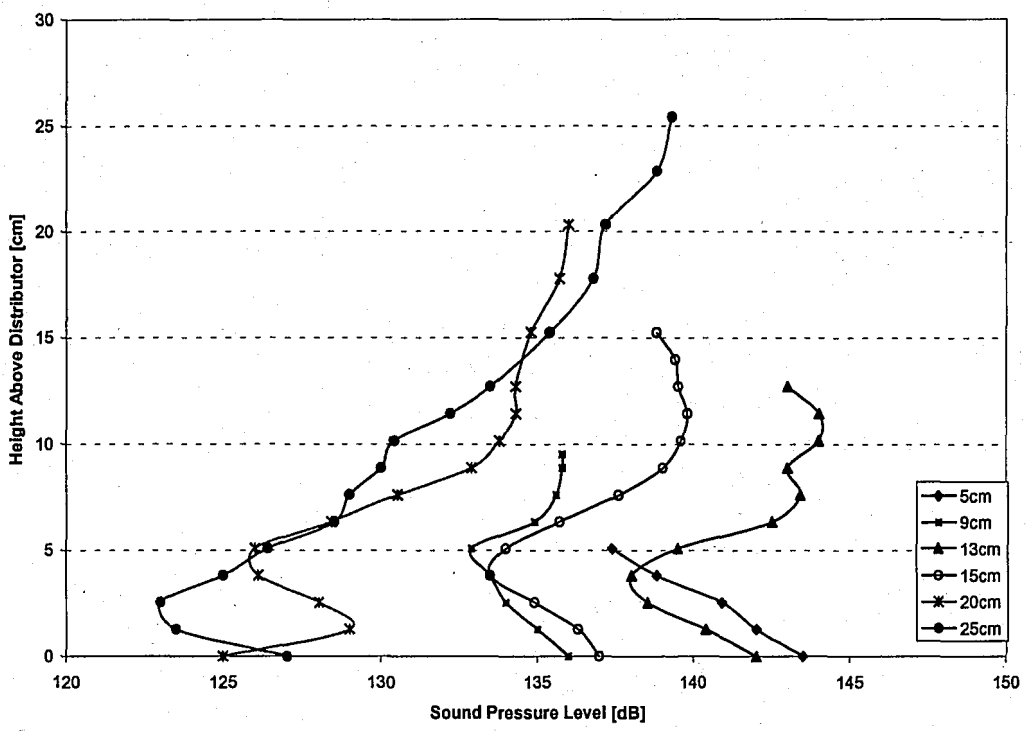

Figure 2.15: Standing Waves for All Tested Bed Depths at 80 Hz

Selecting a Distributor Material

The distributor material is the only remaining design parameter. Other fluidized beds in the Energy Research Center's Fluidization Laboratory use either a sintered glass or a sintered steel plate as a distributor. As an alternative, packed beds of steel beads and sand were tested to observe the fluidization conditions they produced. For the tests, a small layer of the sand or beads was placed atop the sintered glass distributor in the 6-inch cylindrical bed shown in Figure 2.16. Fly ash was then added and the fluidization properties were observed.

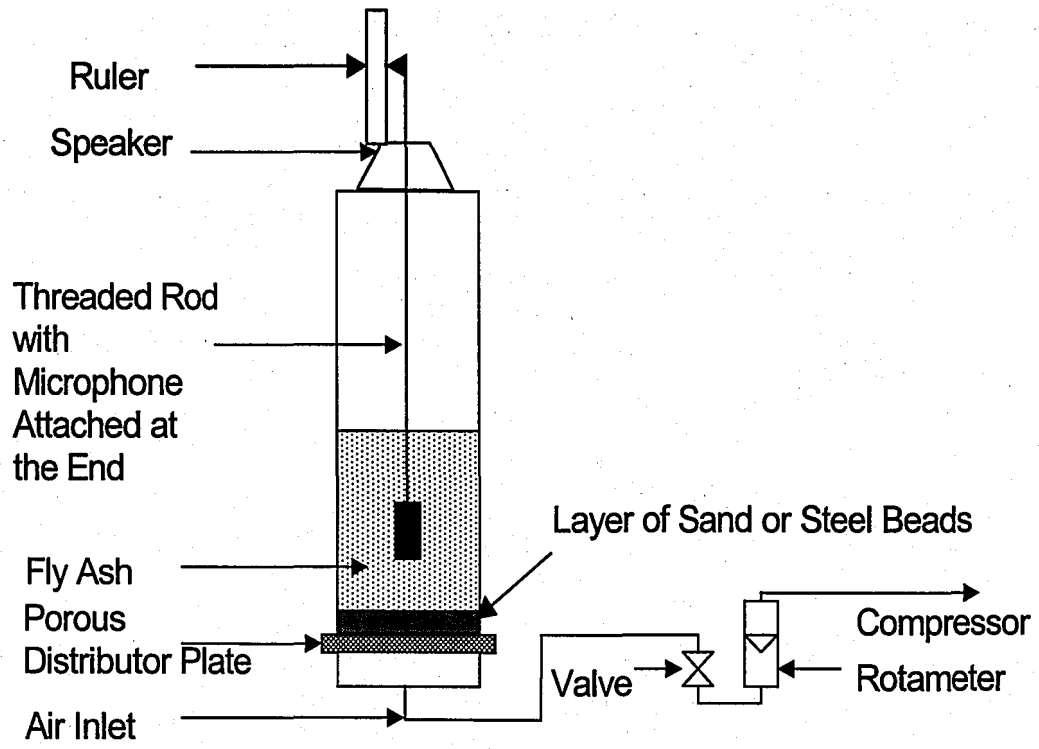

Figure 2.16: Cylindrical Batch Bed Setup With a Layer of Sand or Steel Beads

For this test both Homer City and Baldwin fly ashes were used. The Baldwin ash has a mean particle size of 32 μm and is very difficult to fluidize therefore an acoustic field is necessary. The Homer City and Baldwin ashes achieved good fluidization with the sand and steel bead distributor. Both types of distributor material produced good bubbling and good mixing. For the design of the new bed, the sand was chosen over the steel beads because of its low thermal conductivity. As a result, less of the heat from fly ash will be transferred to the structure of the fluidized bed.

Once the material was chosen, the next step was to observe the acoustic

characteristics of a bed with sand as a distributor. Figure 2.17 shows the standing wave in a bed of just fly ash and then in a bed of fly ash with approximately 2.5 centimeters of sand at the bottom.

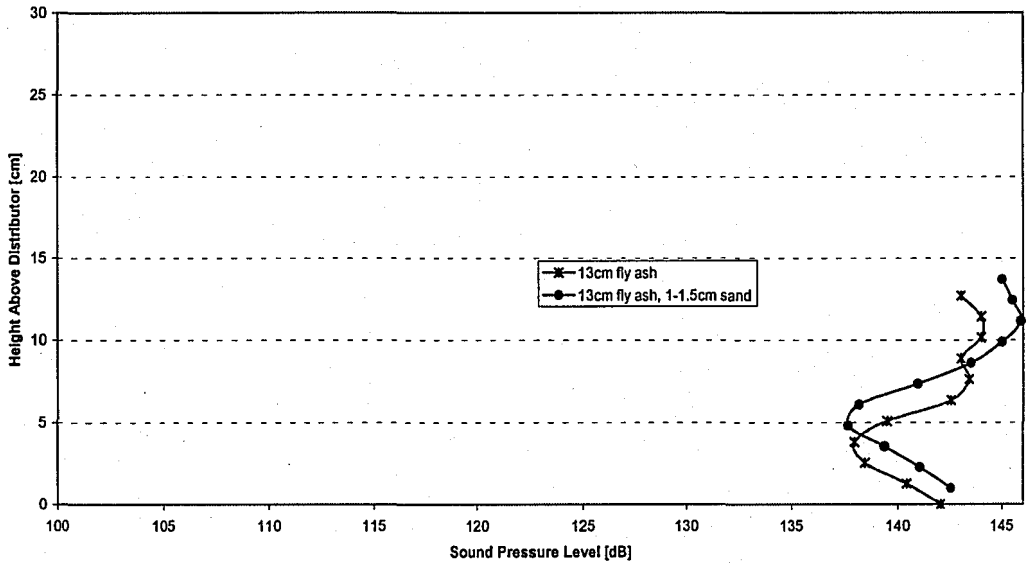

Figure 2.17: Standing Waves in a 13-cm Deep Bed with and without a 1.5-cm Layer of Sand

Both tests yielded essentially the same waveform. Therefore, it was confirmed that the sand would be a good distributor material for the new horizontal fluidized bed.

CHAPTER 3: DESIGN ANALYSIS

The new bed was designed in three sections, the entrance section, the heated section and the cooled section. Each section consists of a plenum and side walls. The plenum and the side walls, with the exception of the side walls in the heated section were constructed of 18 gauge steel. Temperatures reach 399 C in the heated section so the side walls were constructed of 11 gauge steel in order to minimize warping. All of the joints were flanged and bolted together using 5/16" (0.794 cm) hex bolts for ease of assembly and maintenance. A strip of 0.159 cm thick ceramic paper was used in all joints as a gasket material. The properties of this material also help to reduce the heat transfer between sections.

The Plenum Section

The plenum is a closed system for each section so that a one rotameter can measure the flow rate of air to a single section. To enhance the air distribution, two perforated plates were welded horizontally in the plenum. The lower plate was approximately 40% open and the upper plate was approximately 25% open. To ensure that the air did not escape along the sides of the plenum the perforated plates had a 1.25 cm margin with no perforations on all four sides. Figure 3.1 shows the design of the plenum.

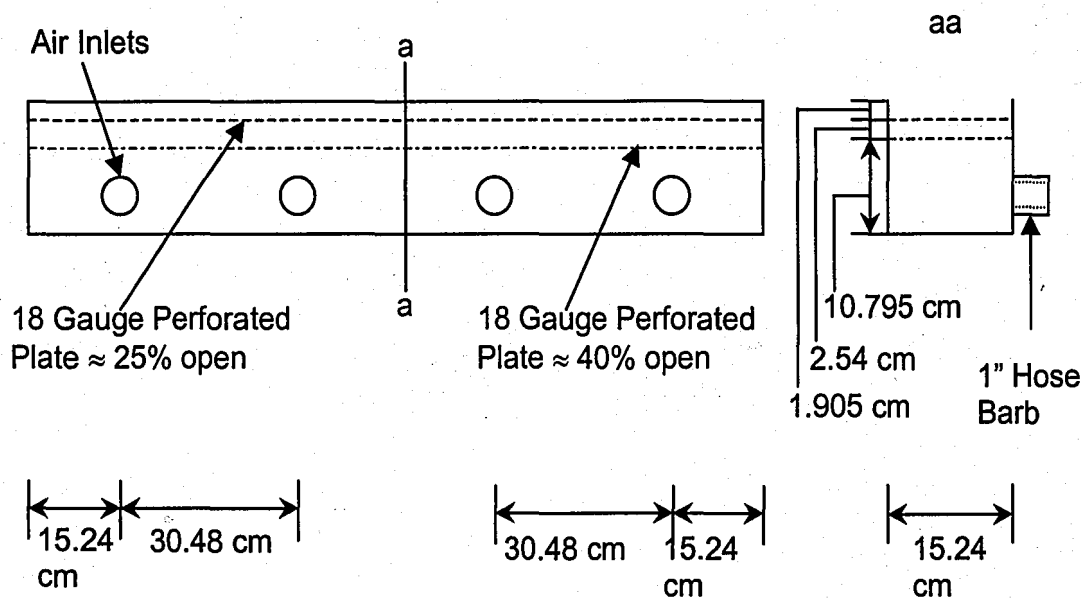

Figure 3.1: Drawing of the Plenum Section

The Heated Section

The next step in the design process was to determine the length and height of each section. The length of the entrance section was not of any consequence, therefore, in order to use a minimal amount of fly ash the entrance section was limited to 0.61 meters in length. The length of the heated section is governed by the number of heaters needed.

Power Requirements. Equation 3.1 was used to calculate the number of watts needed to heat the fly ash from 21 to 399 C.

$$\dot{Q} = \dot{m} c_p \Delta T \tag{3.1}$$

where c_p is the specific heat of the ash, assumed to be 0.83736 kJ/kg C, $\dot{m}$ is the mass flow rate and ΔT is the change in temperature. For this application the cartridge heaters will need to dissipate approximately 17000 Watts of power. The manufacturer limits the internal temperature of the heaters to 871 C. Dividing equation 2.1 by the number of heaters and solving for T_s gives

$$T_s = \frac{q}{hAn} + T_\infty \tag{3.2}$$

where q is the heat transfer rate, h is the heat transfer coefficient, A is the surface area of the heater, T_∞ is the temperature of the fly ash, n is the number of heaters and T_s is the surface temperature of the heater. It was assumed that the internal temperature of the heater was comparable to the surface temperature and that each heater would dissipate an equal number of watts. Each heater was assumed to have diameter of 1.27-cm and a 15.25-cm heated length. Figure 3.2 shows of plot of the surface temperature versus the number of heaters. To keep the surface temperature well below the manufacturer's limit, 65 heaters were used, with each heater dissipating 260 W.

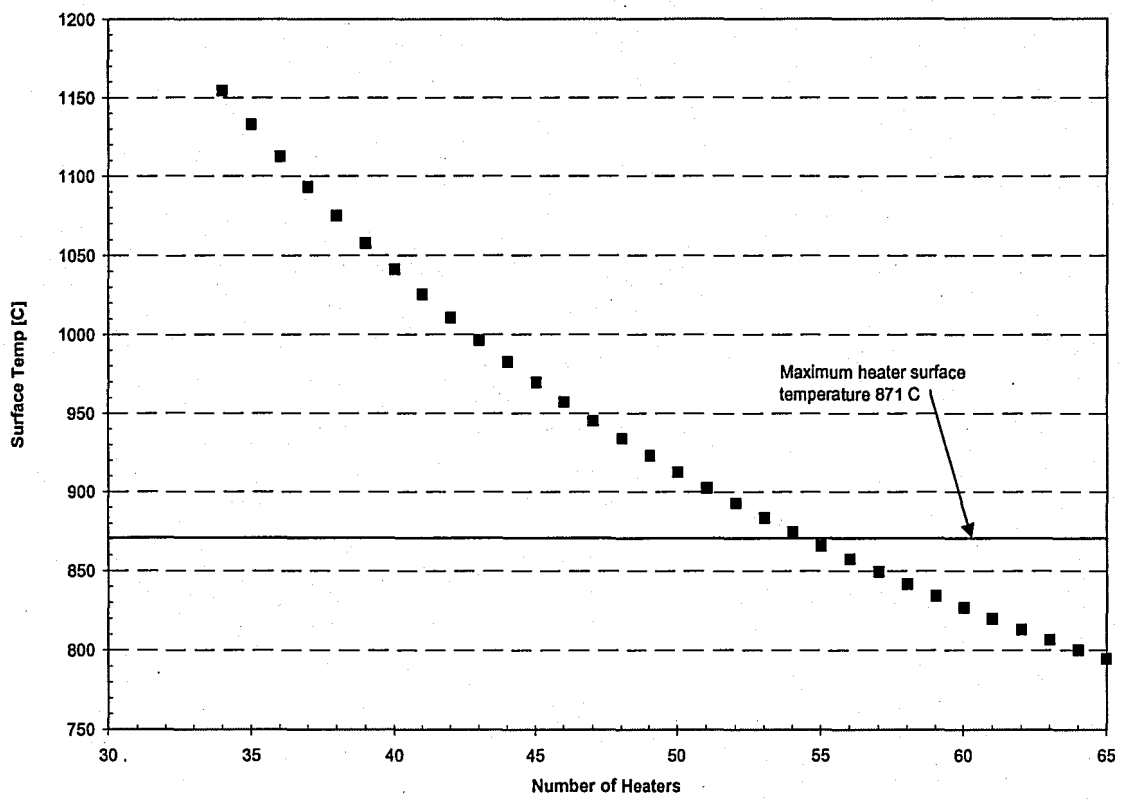

Figure 3.2: Surface Temperature of the Heaters vs the Number of Heaters

To allow for future changes the design allows for 90 heaters. Since the heater spacing is 5.1 cm on center and the bed will operate with a fly ash depth of 13 cm, two heaters can be placed in every column. To get 90 heaters the bed will need to have 45 columns and therefore the heated section length needs to be 182.88-cm. A dam was installed at the end of the heated section to control the upstream bed depth. The height of the dam is 13 cm.

The Cooled Sections - Heat Exchanger Analysis

After the fly ash reaches 399 C it is cooled to 93 C by a heat exchanger consisting of 1.27 cm diameter tubes oriented perpendicular to the ash flow. The NTU method was applied for a cross flow heat exchanger with the fly ash mixed

and the cooling air unmixed in order to find the number of tubes necessary to cool the ash to 93 C. For this type of heat exchanger the effectiveness relationship is:

$$\varepsilon = \left(\frac{1}{c_r}\right)\left(1 - \exp\left\{1 - c_r\left[1 - \exp(-NTU)\right]\right\}\right) \tag{3.3}$$

where ε is the heat exchanger effectiveness, NTU is the number of transfer units and C_r is the capacity rate ratio

$$C_r = \frac{C_{\min}}{C_{\max}} \tag{3.4}$$

For this heat exchanger

$$C_{\min} = \dot{m}_h c_{p,h} \tag{3.5}$$

and

$$C_{\max} = \dot{m}_c c_{p,c} \tag{3.6}$$

where $\dot{m}_h$ is the mass flow rate of the fly ash, $\dot{m}_c$ is the mass flow rate of the air and $c_{p,h}$ and $c_{p,c}$ are the specific heats of the fly ash and the air respectively. In order to solve Equation 3.3 for NTU, the effectiveness must first be found with

the relationship

$$\varepsilon = \frac{C_{\max}\left(T_{c,o} - T_{c,i}\right)}{C_{\min}\left(T_{h,i} - T_{c,i}\right)} \tag{3.7}$$

where $T_{c,o}$ and $T_{c,i}$ are the output and input temperatures of the cooling air respectively and $T_{h,i}$ is the initial temperature of the fly ash. In order to find the number of tubes needed to cool the ash the total area of the heat exchanger must be found. First, the overall heat transfer coefficient must be calculated. This can be found by solving

$$U = \frac{1}{\left(\frac{1}{h_h} + \frac{1}{h_c} + \cancel{\frac{l}{k}}\right)} \tag{3.8}$$

where l is the thickness and k is the thermal conductivity of the pipe wall. Also h_h and h_c are the local heat transfer coefficients of the fly ash and the air respectively. The conductive term has been neglected by assuming that the wall is sufficiently thin. The heat transfer coefficient of the fly ash is known from previous experiments. Since the airflow through the tubes is turbulent, with a Reynolds number of approximately 8.5×10^3, the heat transfer coefficient of the air can be approximated by

$$h_c = 0.0144 c_{p,c} \frac{\left(\frac{\dot{m}_c}{A_T}\right)^{0.8}}{D^{0.8}} \tag{3.9}$$

where A_T is the total area of the heat exchanger and D is the diameter of the heat exchanger tubes. Since the total area of the heat exchanger is unknown, Equation 3.10 must be solved through trial and error with the limiting case that the length of the tubes must be 15.24-cm.

$$NTU = \frac{A_T U}{C_{\min}} \tag{3.10}$$

After finding the total area of the heat exchanger the number of tubes can be found by solving Equation 3.11 for n.

$$A_T = \frac{n\pi D^2}{4} \tag{11}$$

Figure 3.3 shows the number of tubes calculated with Equation 3.11 and the air velocity calculated with Equation 3.9. From this analysis the heat exchanger needs 265 tubes.To make fabrication easier 266 tubes will be used.

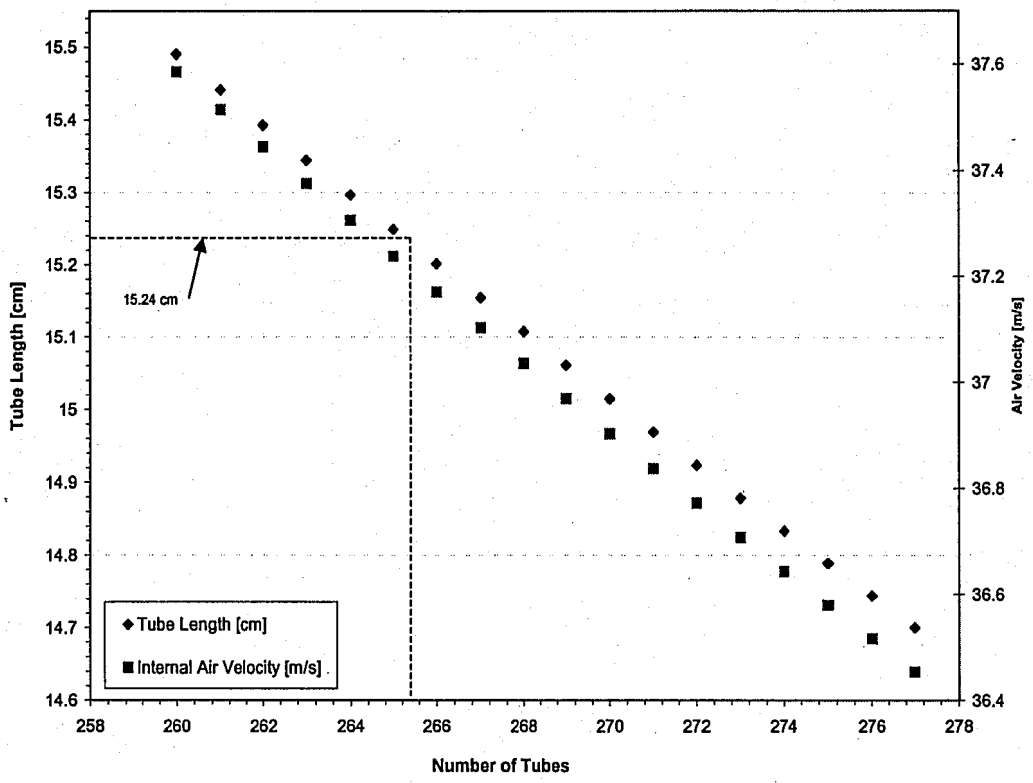

Figure 3.3: The Number of Tubes Necessary to Sufficiently Cool the Ash

The ash-side heat transfer coefficient is relatively constant in the range where the tubes are spaced 4.45-6.35-cm apart as shown by previous experiments. In order to make the cooled section as compact as possible the tubes are spaced 4.45 cm apart. With 3 tubes in each column, all 266 tubes will fit into two 182.88 cm long sections. Each cooled section is the same length as the heated section. The only dimension left to find is the height of the bed.

Height of the Bed

The distance from the free surface to the speakers depends on the frequency of sound needed for operation. Also, in the existing inclined bed, the frequency is fixed for a fixed bed depth because the height cannot be changed.

In the new bed, the top plate to which the speakers are mounted is bolted to the side walls instead being permanently attached. From previous experiments, the operating frequency is 80-Hz. From equation 2.2. the speakers are located 107.19-cm above the free surface. Since the operating bed depth is 13 cm, the side walls need to be 120.19 cm tall. To make the bed as flexible as possible the side walls are only 114-cm tall. The remaining height was gained by installing wooden strips between the side walls and the top plate. This allows the operating frequency to be changed for a fixed bed depth.

The heaters used in the bed have a total length of 20.32-cm with 5.08-cm non-heated section on the end with the leads. That end also has a 3/8" (0.953 cm) male NPT fitting which screws into a 3/8" (0.953 cm) NPT half-coupling welded onto the bed wall. Figure 4 illustrates the heater design.

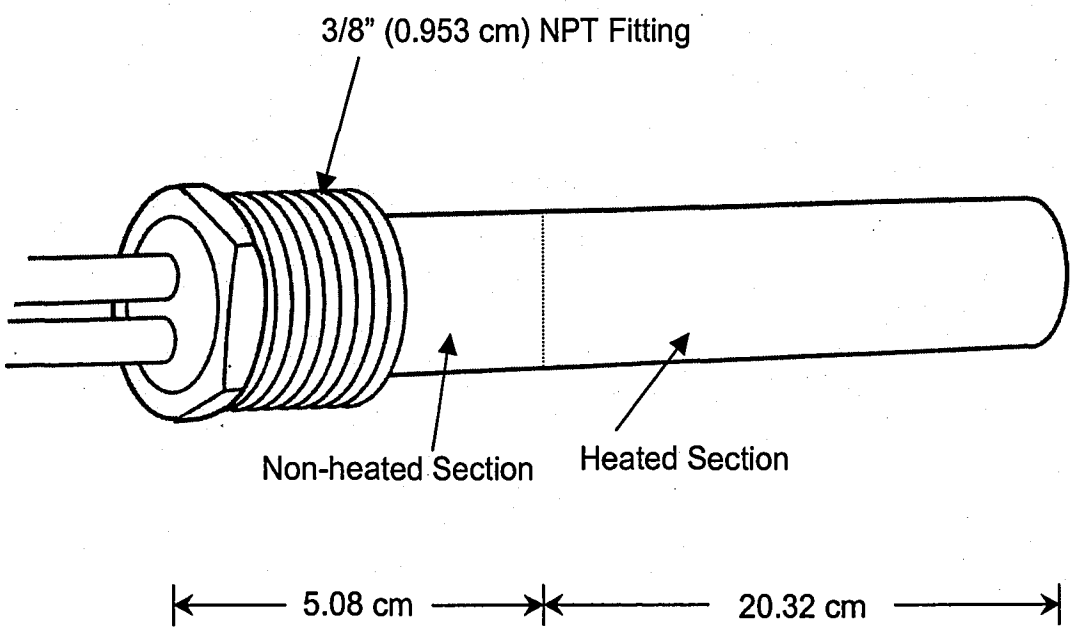

Figure 3.4: Cartridge Heater Used in the Heated Fluidized Bed

To supply electricity to the 208V heaters, a transformer was used to step down the voltage in the laboratory from 600V three phase to 208V three phase. Power to the heaters is controlled by contactor boxes and is distributed to the individual heaters by terminal strips.

Air for the cooling tubes is provided by a fan. Opening or closing a louvre controls the flow rate. A section of duct had to be constructed to take the air from the original ductwork to the cooled sections of the bed. The air passes through the tubes and exits through the other side. Since the operators of the bed will be on the exit side of the bed an air diverter was installed to direct the air upward.

The process of fluidizing the fly ash creates large amounts of dust inside the chamber. To remove the dust and the ammonia released from the contaminated fly ash, a venting system has been installed. At three places in the bed, dust and ammonia are removed, filtered to remove the dust and then vented outside. A fan draws the ammonia and dust through the ducting.

Instrumentation

To monitor and control the system several instruments are needed. To control the heaters a Watlow 145D-1603-1000 High Limit Control and a Fuji PXW4-RAY1-4V Process Control have been installed. The high limit control is connected to a thermocouple installed on the inside of one of the heaters by the manufacturer. If the temperature of that heater goes above the set limit then

power to all heaters is shut off. A thermocouple measuring the temperature of the fly ash is connected to the process control. This turns the heaters on and off to keep the fly ash at the desired temperature. Thermocouples were also installed at various places in the heated section and the cooled section to monitor fly ash and air temperatures. These thermocouples were connected to a digital thermometer so that the readings could be recorded. Three other heaters also have internal thermocouples which are connected to the digital thermometer. Dwyer model RMC flowmeters with brass bottom mounted valves, measure and control the fluidizing air flow rate. Table 3.1 summarizes the bed dimensions and process conditions. Figure 3.5 shows the CAD drawing of the fluidized bed.

Internal Bed Width	15.24 cm
Bed Height (Distributor to Speakers)	120.19 cm
Expanded Bed Depth	13 cm
Mass Flow Rate of Ash	226.8 kg/hr
Superficial Air Velocity at 25 C	2.96 cm/s
Heated Ash Temperature	399 C
Cooled Ash Temperature	93 C
Heated Section	
Length	1.83 m
Number of Possible Heaters	90
Number of Heaters Used	61
Length of Heater	heated length 15.24 cm overall length 20.32 cm
Heater Spacing	Staggered Array, 5.1 cm apart
Heater Diameter	1.27 cm
Heater Power	208 V, 260 W
Cooled Sections	
Number of Cooled Sections	2
Length Per Section	1.83 m
Total Number of Cooling Tubes	266
Tube Spacing	In-line Array, 4.45 cm apart
Diameter of Tubes	1.27 cm
Sound System	
Amplifiers	(5) Kenwood KR-A5070
Speakers	(20) 8" 100 W Subwoofers
Sound Pressure Level	138 dB

Table 3.1: Summary of the Dimensions and Process Conditions for the New Bed Design

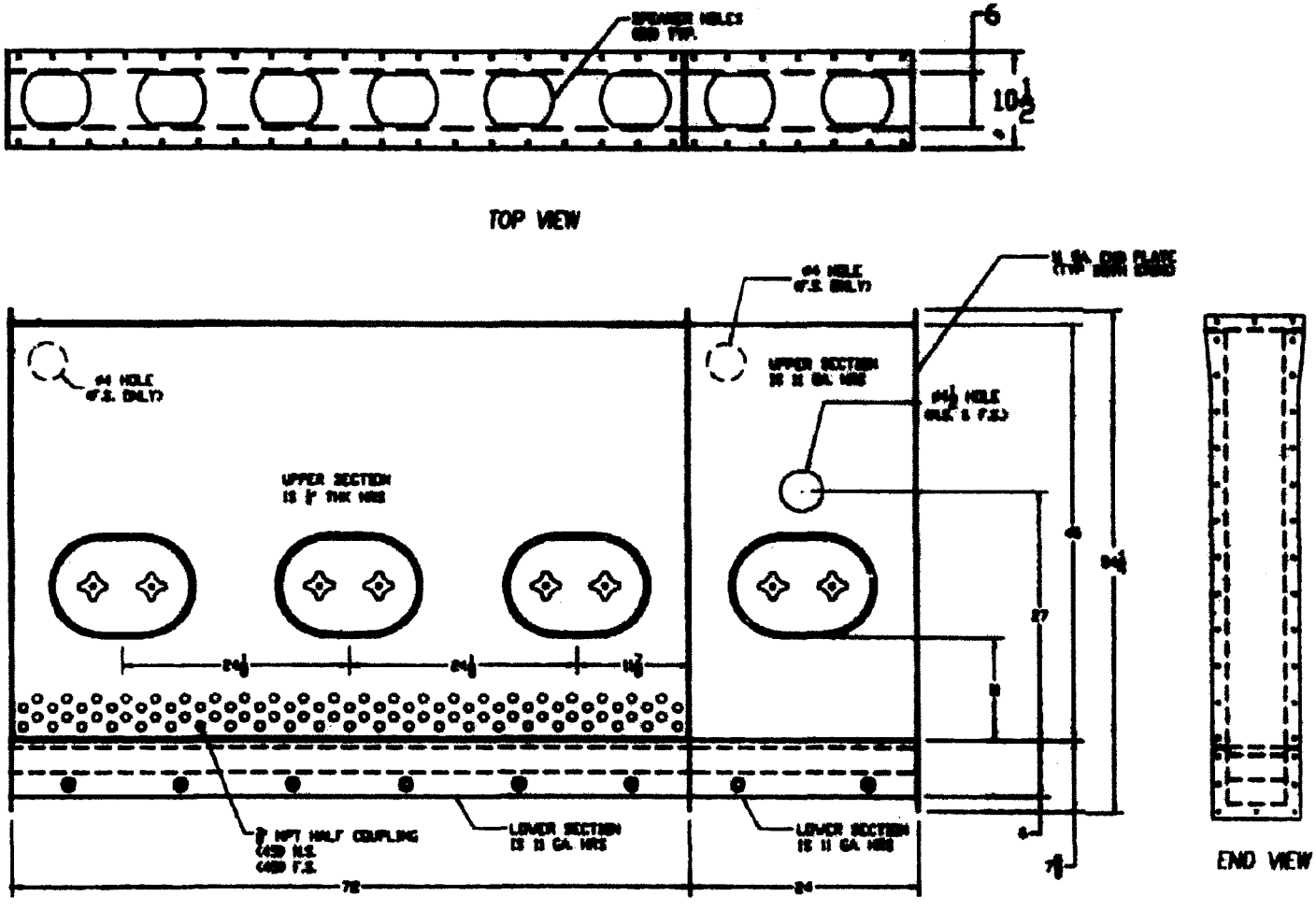

Figure: 3.5a: CAD Drawing of Heated and Entrance Sections

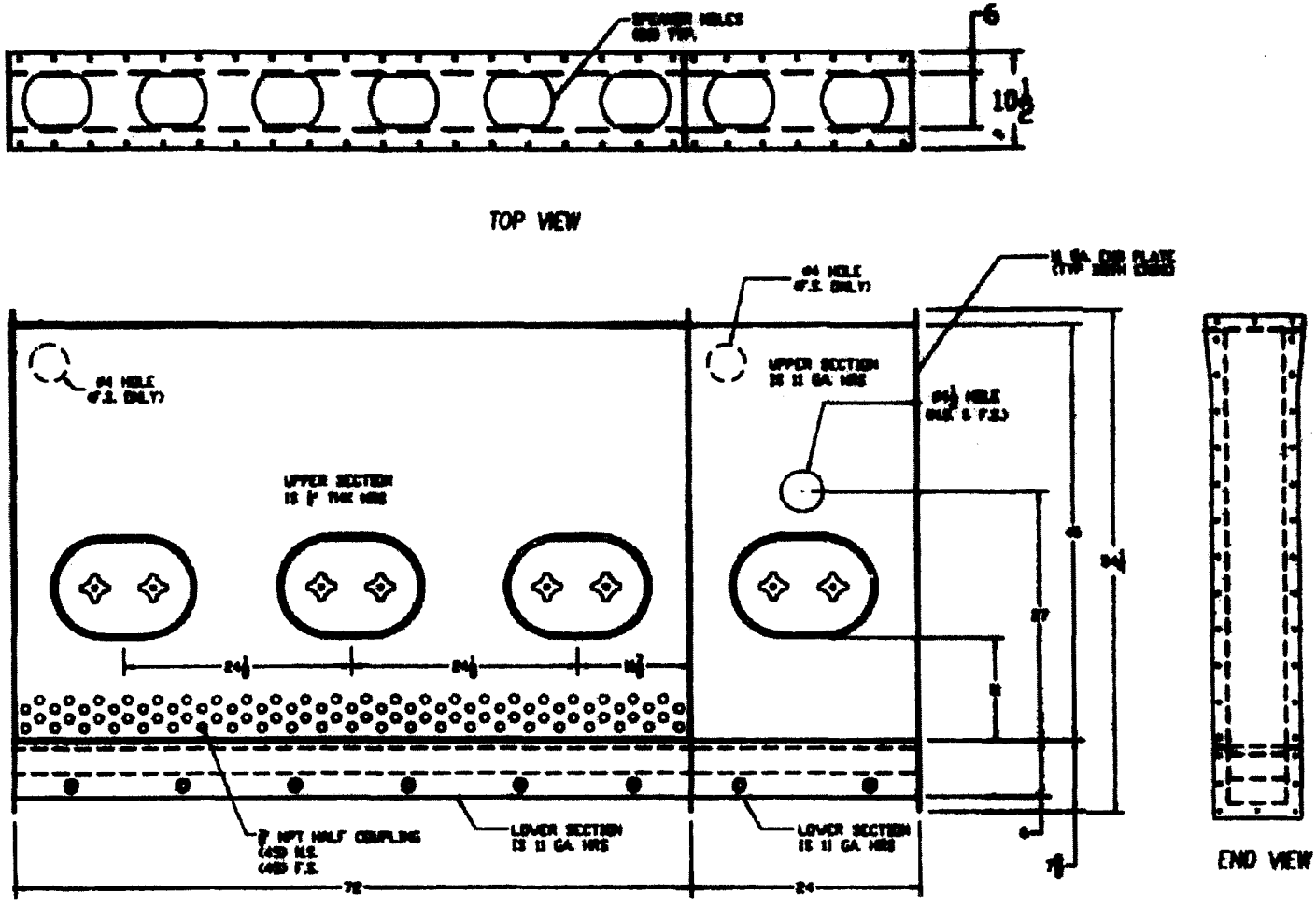

Figure: 3.5a: CAD Drawing of Heated and Entrance Sections

CHAPTER 4: SYSTEM OPERATION

Two different fly ashes were used for the tests in this chapter. Homer City fly ash with a mean particle diameter of 76 μm was used in all tests, except the ammonia removal tests. This ash was chosen for these tests because it was very easy to fluidize. The ash used in the ammonia removal tests was from Nanticoke Station and had a mean particle diameter of 30 μm.

Initial Testing and Modifications

After the new bed was constructed, the first experiments were designed to test the operation of the bed. The first test was to observe the fluidization conditions. For this test, Homer City ash with a mean particle diameter of 76 μm was used. First, the fluidizing air was turned on and then the screw feeder. After several minutes, the air and screw feeder were shut off and the bed was accessed by opening the port covers in the side wall. The ash should have been fluidized and flowed horizontally down the bed until it reached the dam separating the heated section from the cooled section. However, the ash accumulated into a pile just below the screw feeder. After several more tests at various fluidization velocities it was found that a much higher air velocity was needed to achieve fluidization. To achieve good fluidization and good mixing, an air velocity of 2.96 cm/s was needed. This velocity is much larger than the 1 cm/s needed in the other fluidized beds at the Energy Research Center. Even though good mixing and fluidization were achieved, the fluidization was unstable. When

an area in the bed had a buildup of fly ash, that area became defluidized. To solve this problem modifications were made to the bed.

One cause of the unstable fluidization was the air distribution system. In the other fluidized beds at the Energy Research Center, a sintered material was used as a distributor to evenly distribute the air. The sintered material produced a high pressure drop which assured even air distribution. In the new setup, sand was used in place of the sintered material and did not produce sufficient pressure drop. Hence, when fly ash was introduced into a section, instead of the ash being fluidized the air followed the path of least resistance. Therefore, some areas of the bed became defluidized. To remedy the situation the distributor section was subdivided into smaller sections to better control the air distribution. Good fluidization had been achieved in the entrance section . This section has a length of 0.6096 m. Therefore, the heated section was divided into three 0.6096 m sections. To make these modifications, an access panel was cut into the side wall of the plenum with a plasma cutter. Figure 4.1 shows the modifications. Two steel plates were installed at each cutout. One plate was installed in the bottom between the bottom of the plenum and the lower perforated plate. A second plate was installed between the two perforated plates. High temperature caulk was used to seal around the edges. All of the sealed edges were tested for leaks, but not all of the leaks could be sealed due to the original construction of the plenum. Small amounts of air still leak through the joints. A cover plate was installed over the cut out and it was sealed with high temperature caulk. Three

rotameters now measure the air flow rate into the heated section.

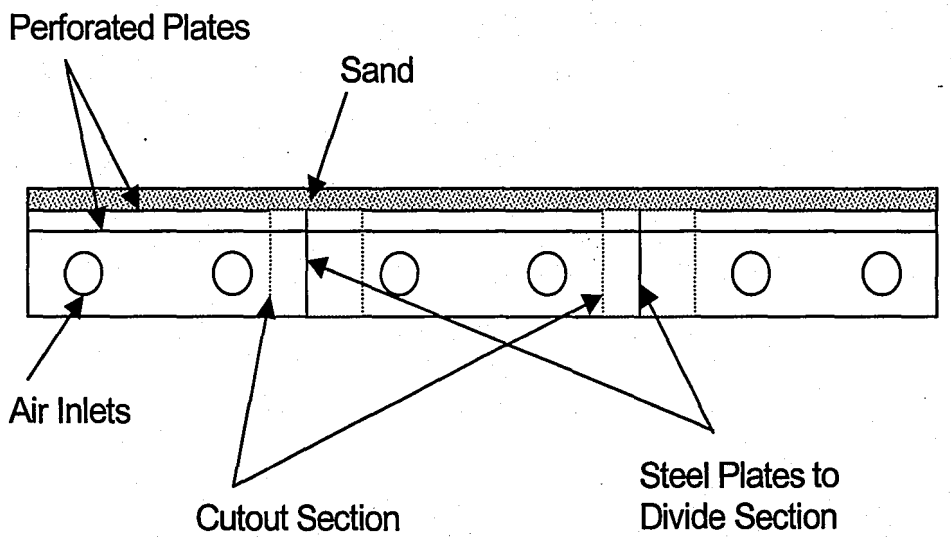

Figure 4.1: Sketch of Modifications Made to the Plenum Section

Once the modifications were made, the fluidization conditions were checked. The fluidization stability was improved and these modifications were then made to the cooled sections as well.

Further testing showed that the fluidization was still not suitable for continuous operation. When the acoustic field was applied, the instability returned and areas of the bed became defluidized. The problem stemmed from the high gas velocities needed for good fluidization. When a buildup of ash in a particular area occurred, some air was diverted to an area with less ash. This caused the air velocities in those areas to be very high. The sand was displaced leaving nothing to distribute the air. Once this happened the only way to fix the

problem was to remove all of the fly ash and sand and install a new layer of sand. To solve this problem the sand was replaced by 0.5 mm steel beads. The steel beads, because of their high density, are not as easily displaced by non-uniformities in the air velocity. After replacing the sand with the steel beads, the fluidization was again checked with and without sound. Fluidization conditions were now acceptable for operation and the next step in the testing process could be taken.

Measurement of Sound Pressure Levels

The next step in the testing process was to check the acoustic characteristics of the bed. Heating the ash uniformly to 399 C is the key to the ammonia removal. This requires good mixing of the bed material and high heat transfer coefficients at the surface of the heater. Therefore, the sound pressure levels in the heated section are important. For this test, ash was introduced into the entrance section and the heated section. The fluidizing air was turned on at a velocity of 3.39 cm/s and the acoustic field was turned on with a frequency of 78 Hz. A microphone was attached to a threaded rod and inserted into the bed at four locations. To start the test, the microphone was positioned just above the distributor and was then raised at set increments. This process was repeated for all four locations. Figure 4.2 shows the experimental setup.

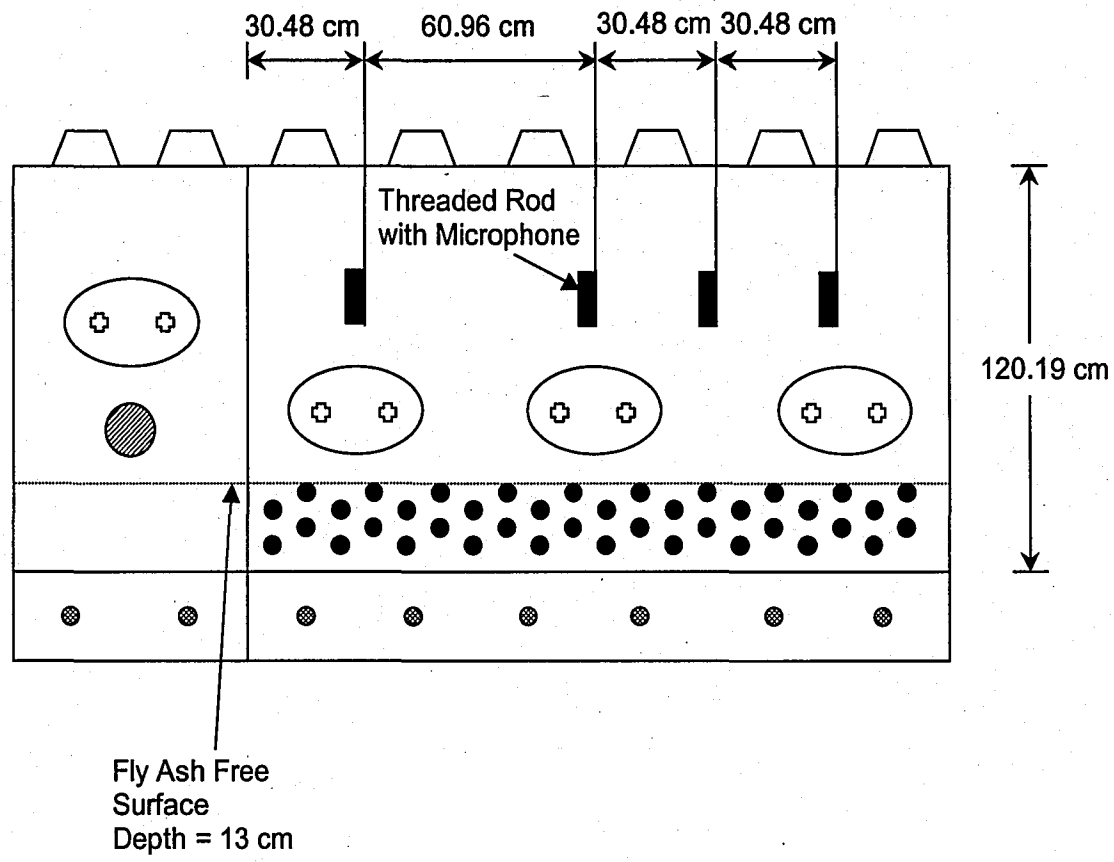

Figure 4.2: Experimental Setup for SPL Measurements

Figure 4.3 shows the waveforms obtained at the four axial positions during the experiments. All of the waveforms are very similar. At the free surface, the SPL ranged from 137 to 140 dB and at the distributor the SPL ranged from 132 to 134 dB. The standing waves for 152.5 cm and 121.9 cm reach lower sound pressure levels just above the distributor.

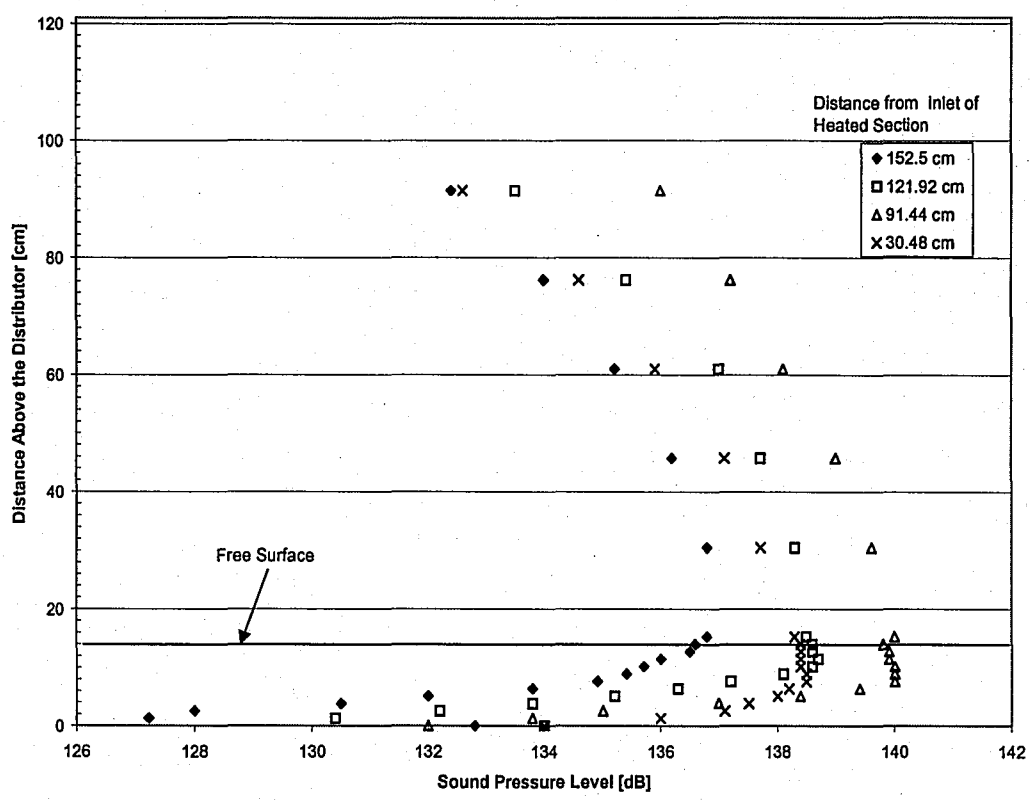

Figure 4.3: Waveforms Observed in the Heated Section

Figure 4.4 shows the sound pressure levels versus the distance from the end of the heated section. Here it is easy to see that the sound pressure level at the free surface and the distributor were approximately the same for all four sampling points. The sound pressure levels for the heated section were sufficient to achieve the fluidization characteristics needed.

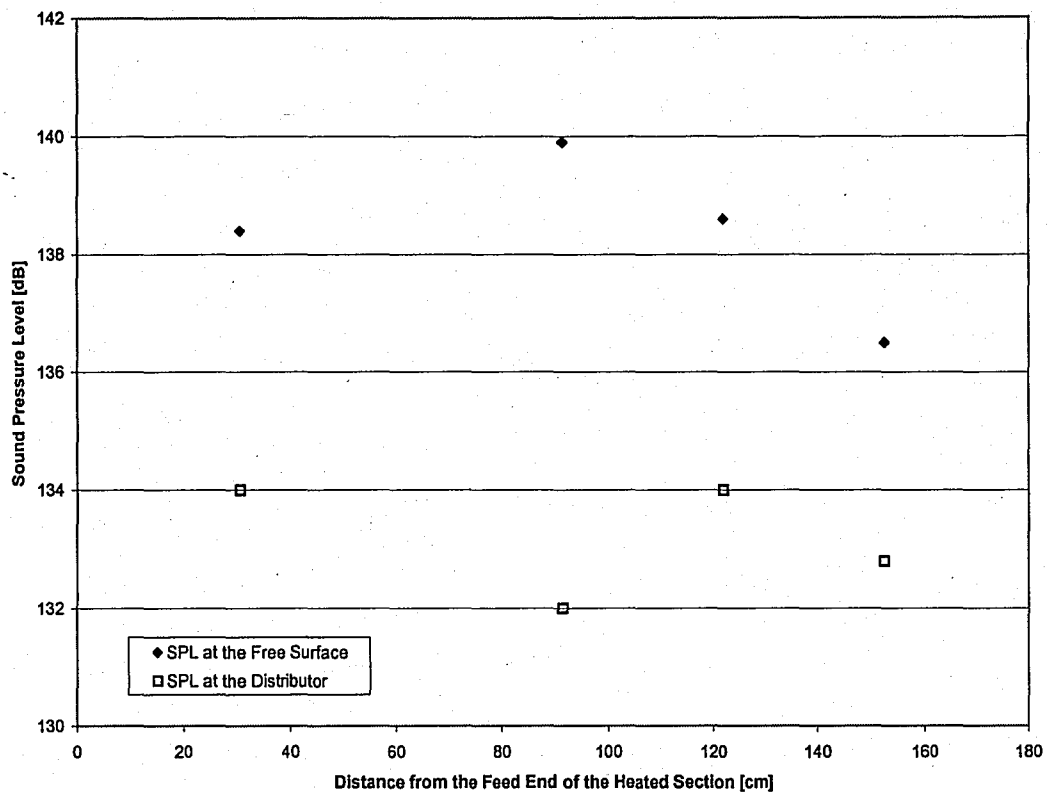

Figure 4.4 Sound Pressure Levels for the Entire Heated Section

Measurement of Ash Temperatures

The next set of experiments was designed to learn about the thermal and dynamic operating characteristics of the bed. For these experiments the entire bed was filled with ash before the start of the test. The fluidizing air and the acoustic field were turned on. Next, the heaters were engaged and the timer started. The process control device was set to keep the ash temperature at 350 C. Temperatures of the ash, the cooling air, both at the inlet and outlet, and the exhaust fluidization air were recorded every 3 minutes. Thermocouples measuring ash temperature were located 7 cm above the distributor and were placed at 0.86, 1.22 and 1.63 m from the inlet end of the heated section and 1.93, 3.14, 4.27, and 5.44 m from the inlet end of the cooled section. The air

temperature for the heat exchanger was also monitored just before the air reached the bed. The final cooling air temperatures were monitored with thermocouples placed at the end of the cooling tube at the same locations as the thermocouples measuring ash temperature. Air temperature was also monitored at the top of the bed just below the speakers and at the exhaust outlet for the heated section. Figure 4.5 shows how these thermocouples were arranged. After the temperature of the fly ash reached the desired level, the screw feeder was turned on at a speed of 20 rpm. The mass flow rate for the experiment was determined by a single timed sample from the outlet of the bed. The mass flow rate for this experiment was determined to be 447 lb/hr. After the fly ash reached its equilibrium temperature the experiment was ended.

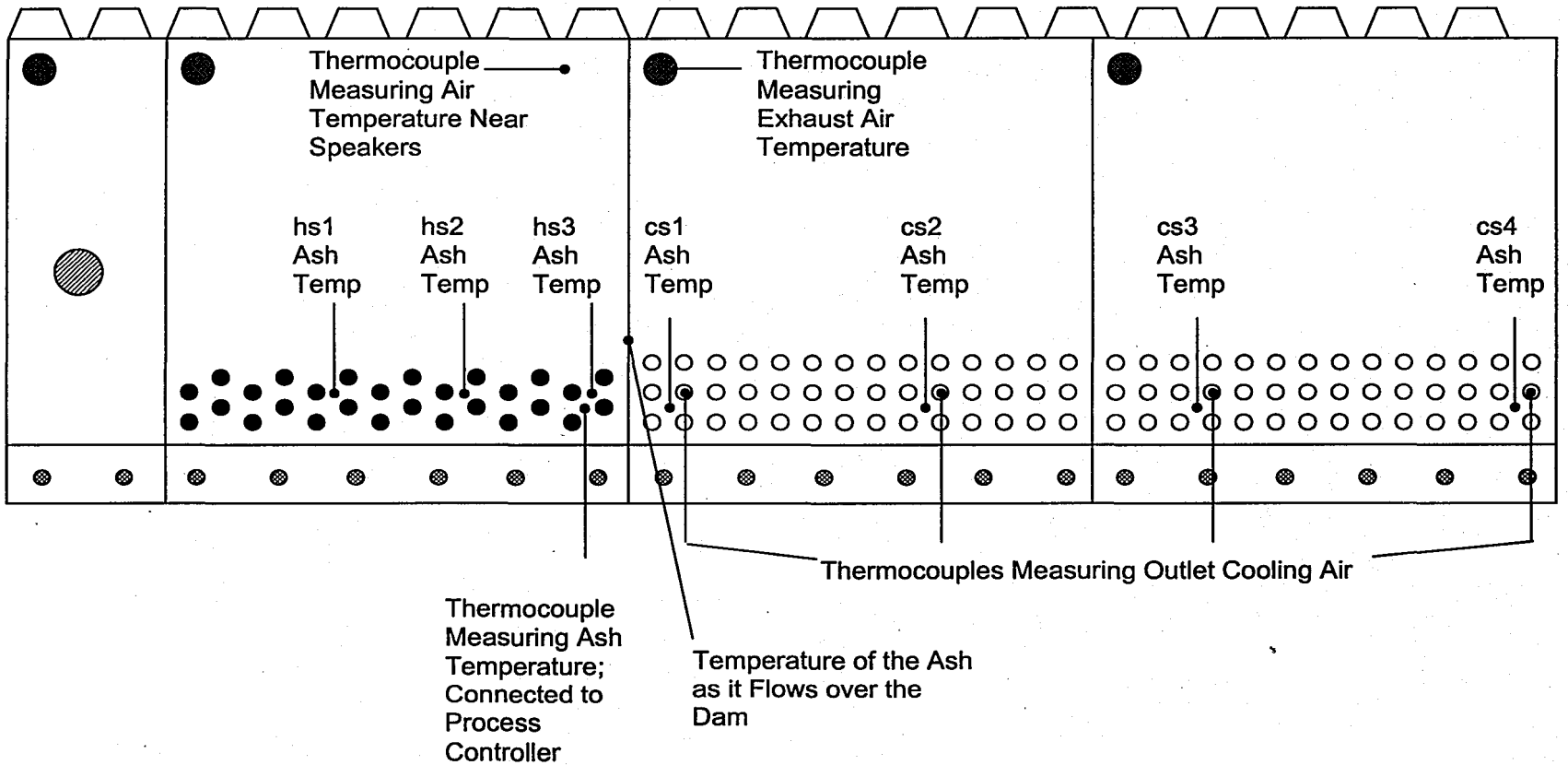

Figure 4.5: Thermocouple Setup in the New Fluidized Bed

Figure 4.6 shows the ash temperatures in the bed for the duration of the experiment. The system takes approximately 18 minutes to heat the ash in the heated section to the desired temperature. At this point the screw feeder was turned on and approximately 12 minutes later the system reached thermal equilibrium. In the cooled section, the ash stayed at the same temperature until the screw feeder was turned on. The ash just over the dam increased in temperature very rapidly once the mass flow was turned on. Temperatures in the rest of the cooled section remained constant.

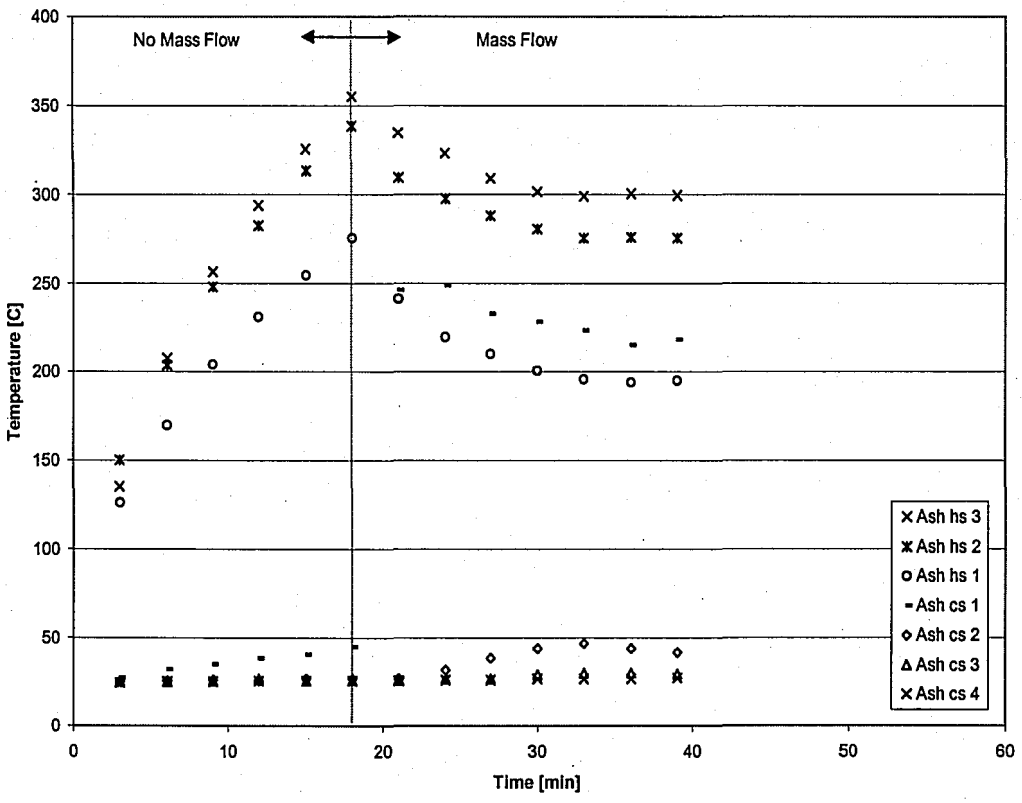

Figure 4.6: Fly Ash Temperatures in the Heated and Cooled Sections

In an attempt to raise the thermal equilibrium temperature at this flow rate, 7 spare heaters are installed into the bed. The experiment was rerun and Figure 4.7 shows the results. The addition of the 7 heaters (1820 W) had little effect on the outcome of the test. The equilibrium temperature for the test with 68 heaters was slightly higher in some locations than the test with 61 heaters.

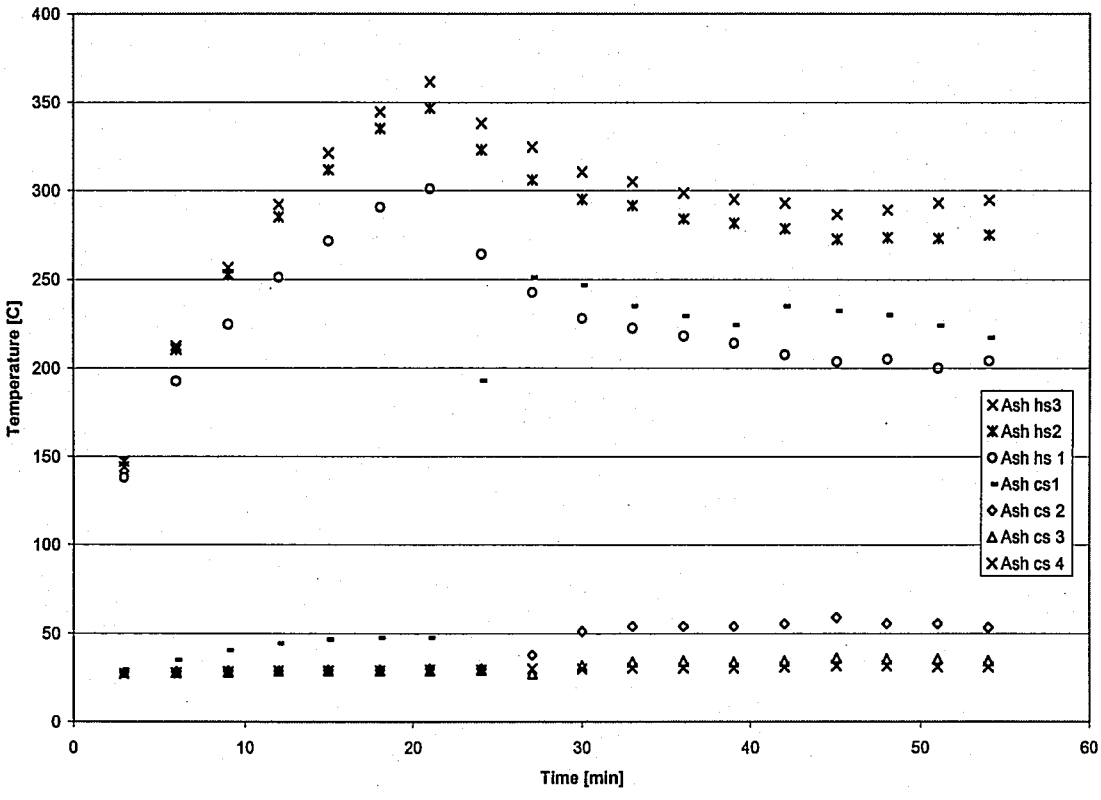

Figure 4.7: Fly Ash Temperature in the Heated and Cooled Sections with 7 Additional Heaters

Figure 4.8 shows the equilibrium temperature distribution in the bed for tests with 61 and 68 heaters. The ash temperatures for this test were slightly elevated in some locations when compared to the previous test.

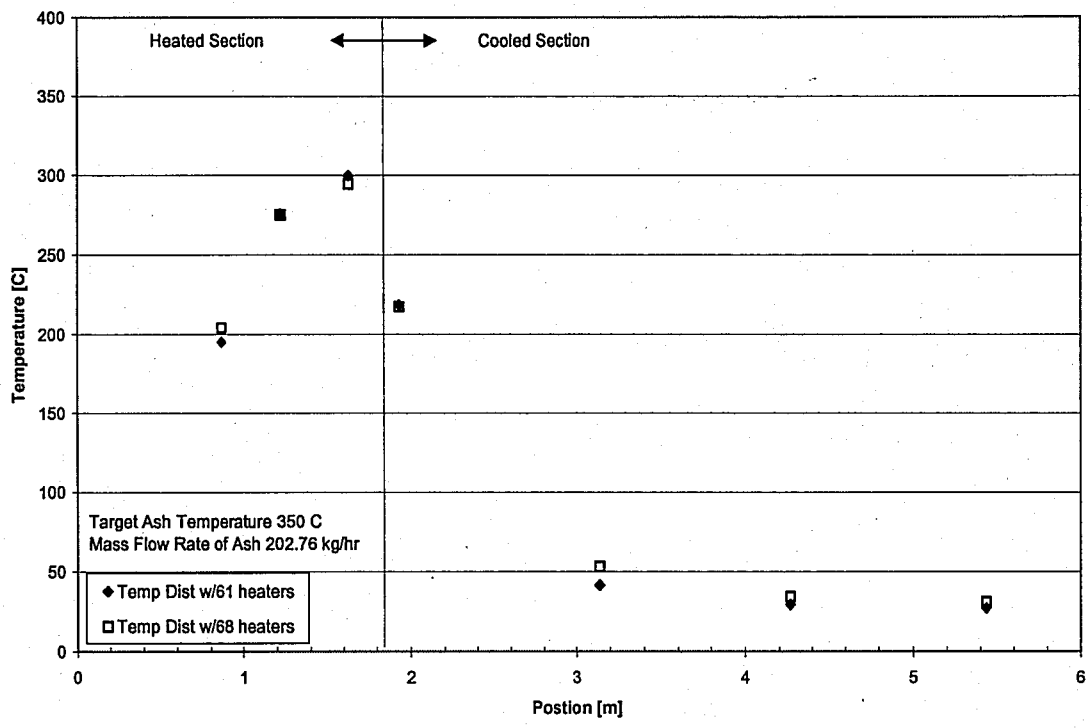

Figure 4.8 Equilibrium Temperature Distribution for the Entire Bed

The next group of experiments was designed to observe the effects of mass flow rate of ash on the system. Ash was again loaded into the entire bed. The fluidizing air and the acoustic field were turned on. The heaters were engaged and the heated section was allowed to heat up to the desired temperature. When that temperature was reached, the screw feeder was turned on and the timer started. Temperatures were recorded every 3 minutes. This test was completed for flow rates of 75.3, 101.2, and 113.4 kg/hr. Flow rate was determined by taking a single timed sample from the ash output. Figures 4.9, 4.10, and 4.11 show these results. From these graphs it can easily be seen that the higher the mass flow rate, the lower the equilibrium temperature of the

system. Furthermore, the system is only able to stay at the desired temperature for approximately 101.2 kg/hr, less than half of the design mass flow rate of 226.8 kg/hr.

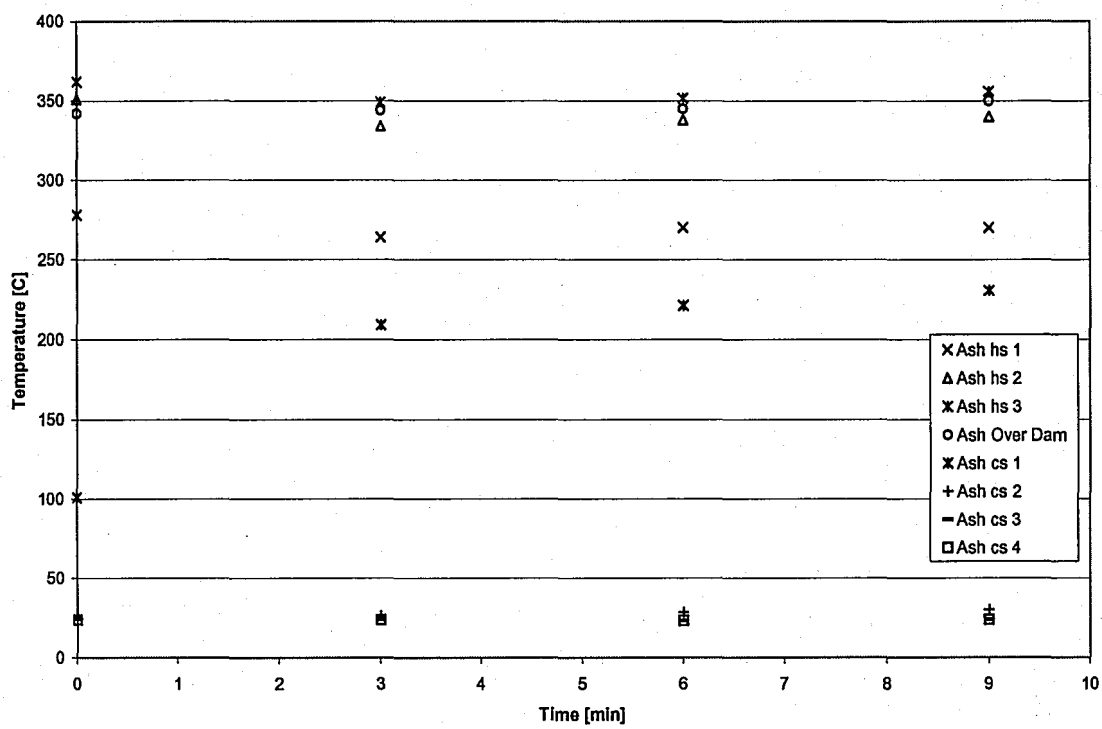

Figure 4.9: Ash Temperatures in the Heated Section with a Flow Rate of 75.3 kg/hr

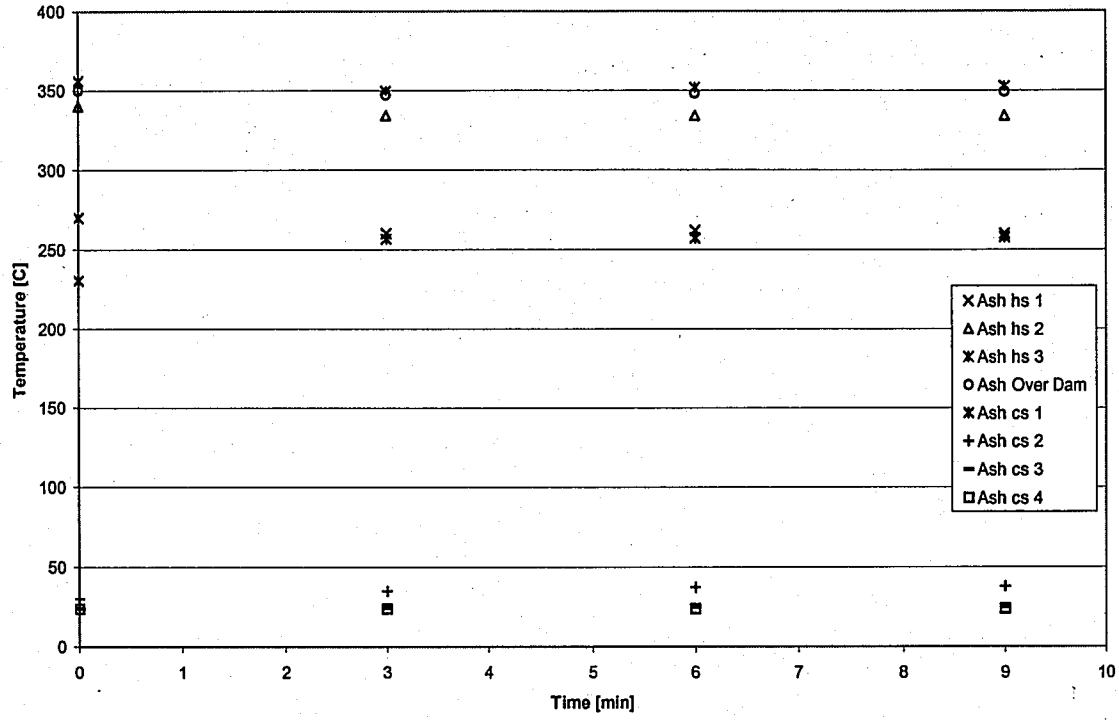

Figure 4.10: Ash Temperatures in the Heated Section with a Flow Rate of 101.2 kg/hr

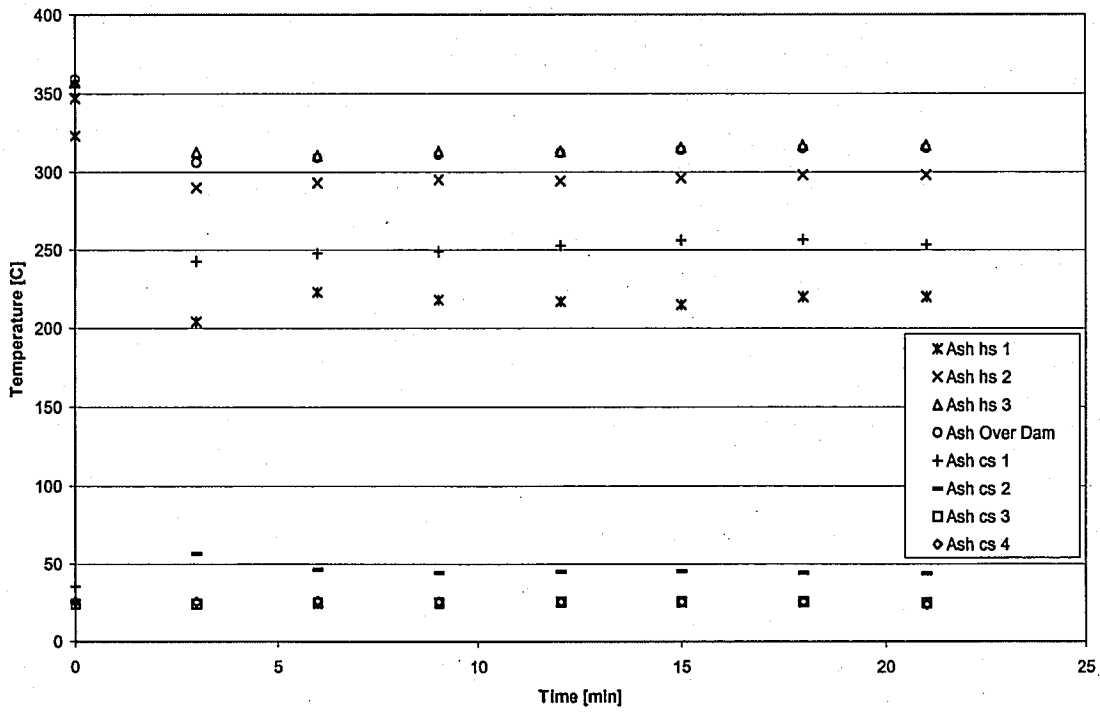

Figure 4.11: Ash Temperatures in the Heated Section with a Flow Rate of 113.4 kg/hr

One possible reason that the heaters were not able to keep up with the design flow rate might be due to the uncertainty of the mass flow measurements made at the discharge end of the bed. Experiments similar to the previous tests were run with the exception that flow rate measurements were taken every 3 minutes along with the temperature measurements. The bed was allowed to return to the desired temperature before the next test was started. Figure 4.12 shows the results from this test. This test shows that the mass flow rate takes approximately 15 minutes from the start of operation to reach equilibrium. The results also confirm the flow rates measured in the previous tests. Therefore, the maximum mass flow rate of the system is less than the design flow rate.

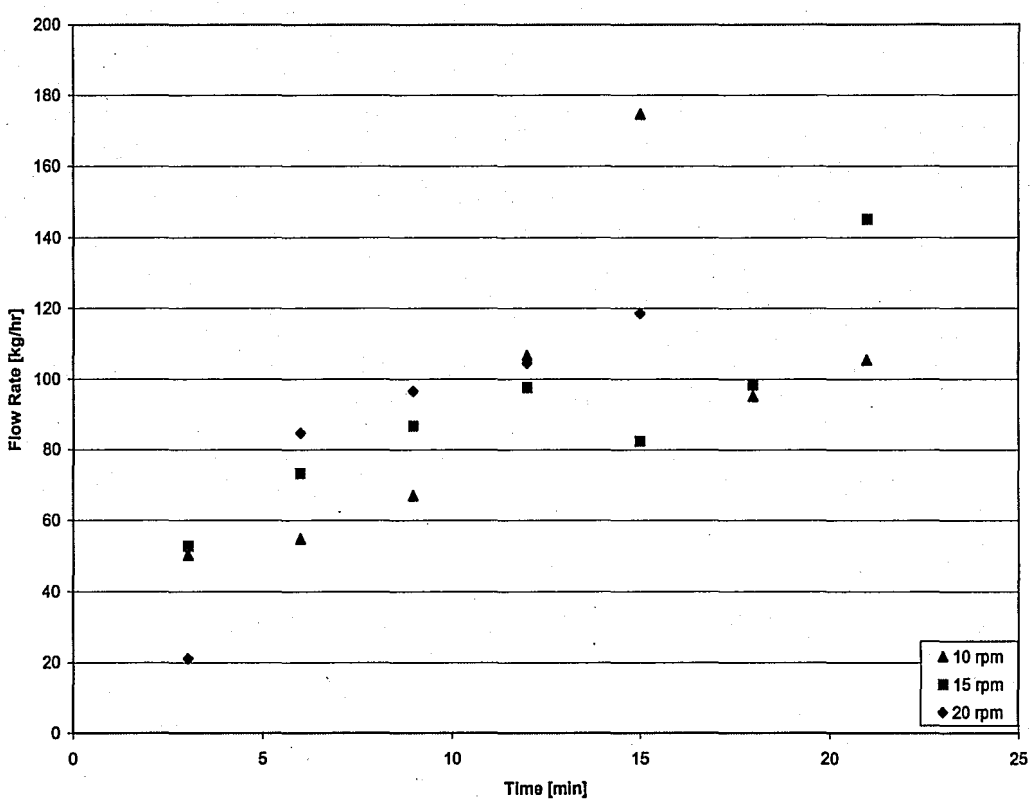

Figure 4.12: Mass Flow Rate Measurements

The same test was again run for the three different screw feeder speeds. However this time, the bed was not allowed to return to the desired temperature before each test. The test was started at a screw feeder speed of 15 rpm. After a sufficient amount of time the screw feeder was increased to 20 rpm. Again, after sufficient time, the screw feeder was reduced to 10 rpm. This test was designed to show the reaction of the system to changes in mass flow rate. The target peak ash temperature of this test was 325 C. Figure 4.13 shows the temperature of the ash in the heated section and the mass flow rate as a function of time. These results show that the mass flow rate of the system, measured at the discharge end, responds very quickly to changes in the screw feeder speed.

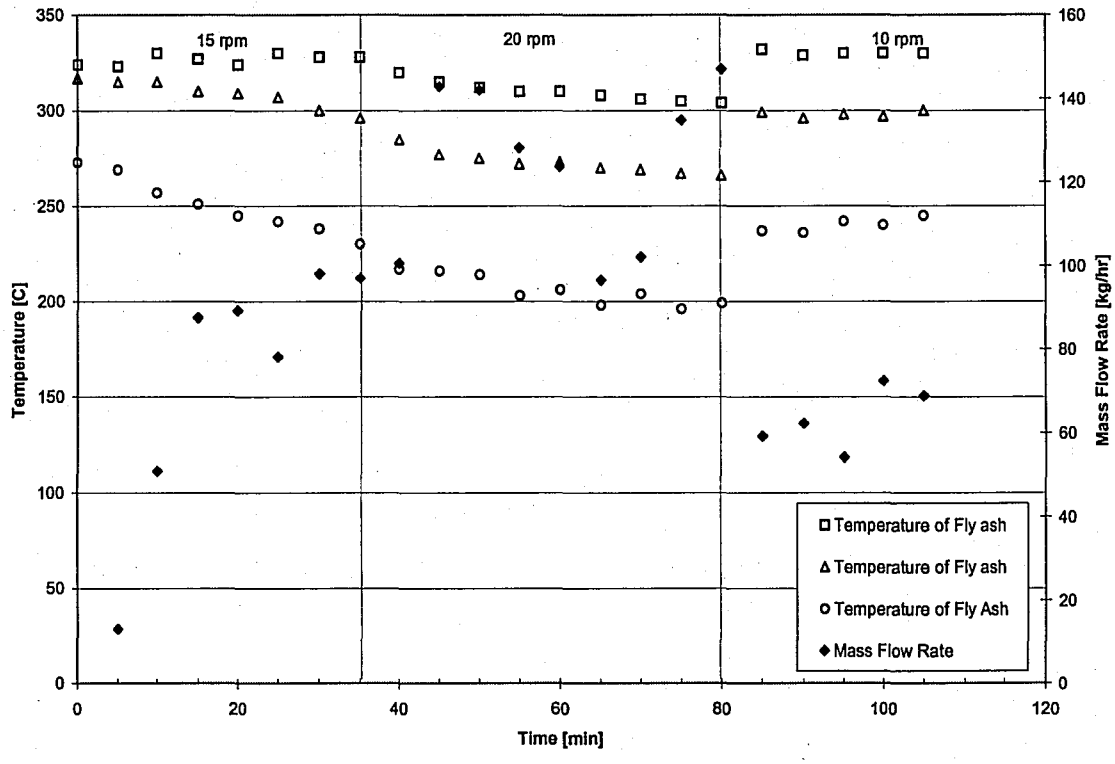

Figure 4.13: Ash Temperature in the Heated Section for Changes in Flow Rate

Tests with Nanticoke Ash

Ash Properties. The next step was to determine the physical properties of the contaminated Nanticoke ash, namely the density, the specific heat, the particle size distribution, the moisture content, the amount of unburned carbon (LOI), and the ammonia concentration. To find the density, a known mass of the ash was placed in a graduated cylinder filled with water. The density of the ash was calculated by dividing the mass of the ash by the change in the volume of water. This experiment was performed several times and the results were averaged. The Nanticoke ash was found to have a density of 1142.66 kg/m^3.

To find the specific heat of the ash, a simple laboratory test was performed. First, a measured quantity of water at room temperature was placed in a calorimeter, a 1.5 liter thermos. Using a thermocouple connected to a digital thermometer the temperature of the water was recorded. Then, a known quantity of fly ash, which had been heated to 90 C in an oven, was added to the calorimeter full of water. The mixture was stirred until an equilibrium temperature was reached. To find the specific heat, Equation 4.1 was used.

$$mc_{ash}\left(T_f - T_1\right) + \left(m_{H_2O}c_{H_2O}\right)(T_f - T_2) = 0 \qquad (4.1)$$

where m is the mass of the fly ash, c_{ash} is the specific heat of the fly ash, T_f is the

equilibrium temperature, T_1 is the initial temperature of the fly ash and T_2 is the initial temperature of the water. Several tests were performed and the specific heat of the fly ash was determined to be between 0.914 and 0.922 kJ/kg C. Coarse and fine fractions of ash from Homer City were also tested. The specific heats for these ashes were found to be 0.842 and 0.906 Kj/kg respectively.

To measure the particle size distribution for the Nanticoke fly ash, a Horiba LA-910 laser scattering particle size distribution analyzer was used. The mean particle diameter was determined to be 29.183 μm.

The moisture content and the LOI of the ash were measured by heating the ash in an oven. First, several small glass crucibles were weighed. Then, the crucibles were filled with the Nanticoke fly ash and then weighed again. They were then heated in the oven at 150 C for 2 hours. The crucibles were weighed again and then heated in the oven at 750 C overnight. The final mass of the crucibles were recorded. Equation 4.2 was used to calculate the moisture content.

$$moisture = \left(\frac{m_{150} - m_2}{m_2 - m_1} \right) * 100 \qquad (4.2)$$

where m_{150} is the mass of the crucible and ash after being heated to 150 C, m_2 is the mass of the crucible loaded before heating, and m_1 is the mass of the crucible. The moisture content of the ash was determined to be 0.076 %.

Equation 4.3 was used to find the LOI of the ash.

$$LOI = \left(\frac{m_{750} - m_{150}}{m_{150} - m_1} \right) * 100 \qquad (4.3)$$

where m_{750} is the mass of the crucible and ash after being heated to 750 C. The amount of unburned carbon in the Nanticoke ash was determined to be 12.56 %.

To determine the ammonia concentration, a known quantity of the ash was placed in a glass jar. Then 100 ml of a 0.2 N sulfuric acid solution (H_2SO_4) was added. After allowing the ammonia to dissolve into the solution for 12 hours, the samples were treated with 3 ml of an ion strength adjuster, ISA, to ensure that the pH of the solution was 12 or greater. A pH of 12 or greater was required to convert all of the aqueous ammonia to gaseous ammonia. Then the ammonia content was then measured using a Fisher 13-620-504 ammonia ion selective electrode. This probe can only detect gaseous ammonia. The probe was connected to a Fisher Accumet AP63 voltmeter and a milli-volt reading was recorded for each sample. A calibration curve was used to interpolate the mole/liter concentration of ammonia in the sample[7]. Equation 4.4 was then used to calculate the ammonia concentration in ppm.

$$ppm = 17000 * \left[\frac{mg_{NH_4}}{mol_{NH_4}} \right] * M \left[\frac{mol_{NH_4}}{lt_{sol}} \right] * \left[\frac{Vol_{sol}[lt]}{Mass_{flyash}[kg]} \right] \qquad (4.4)$$

which reduces to Equation 4.5 in this case

$$ppm = 17000 * \left(\frac{0.1}{Mass_{flyash}[kg]} \right) * M \tag{4.5}$$

where M is the moles/liter of ammonia in the sample solution. The ammonia concentration was found to vary from 750 to 1200 ppm. Table 4.1 summarizes the physical properties of the Nanticoke ash.

Density	1142.66 kg/m^3
Mean Particle Diameter	29.183 μm
Ammonia Concentration	750-1200 ppm
Specific Heat	0.914 - 0.922 kJ/kg C
Moisture Content	0.076 %
LOI	12.56 %

Table 4.1: Physical Properties of the Nanticoke Ash

Ammonia Removal in the Batch Bed. An ammonia removal test was then run in the 15.24 cm cylindrical bed with the Nanticoke ash. Four cartridge heaters were placed 2.54 cm above the distributor. The heaters dissipated a total of 1000 W. Four thermocouples measuring ash temperature were placed along the wall and 2.54 cm above the distributor. A 2 kg sample of the contaminated ash was placed in the bed. Fluidization air and the acoustic field were turned on and

the heaters were engaged. The first sample was taken when the bed reached 148.9 C and were then taken at 28 degree intervals. Samples were obtained by using a long instrument designed to remove samples from the bed. The samples were placed in mason jars to be analyzed for ammonia content using the method discussed previously. Figure 4.14 shows the results of this test. At 365 C the ammonia content of the ash was reduced to a sufficiently low level. The Nanticoke ash used in this test had an initial ammonia contamination of approximately 700 ppm. Figure 4.15 shows the ammonia content as a percent of the initial contamination.

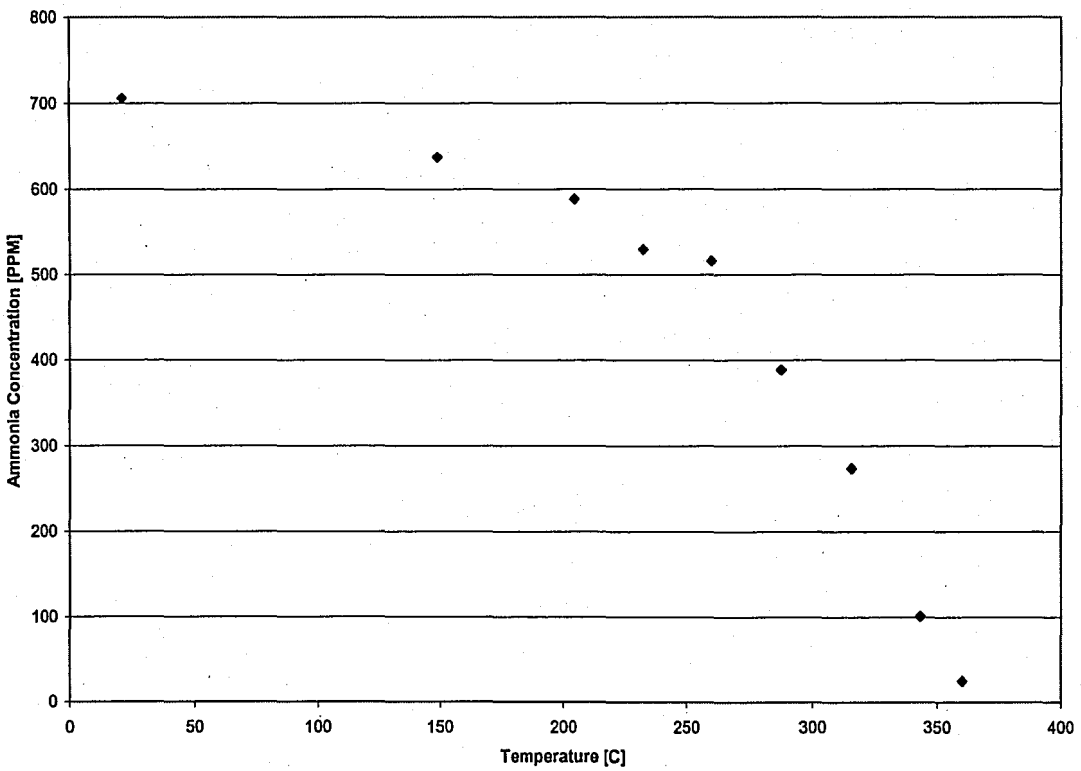

Figure 4.14: Ammonia Concentration of the Ash in the Batch Bed

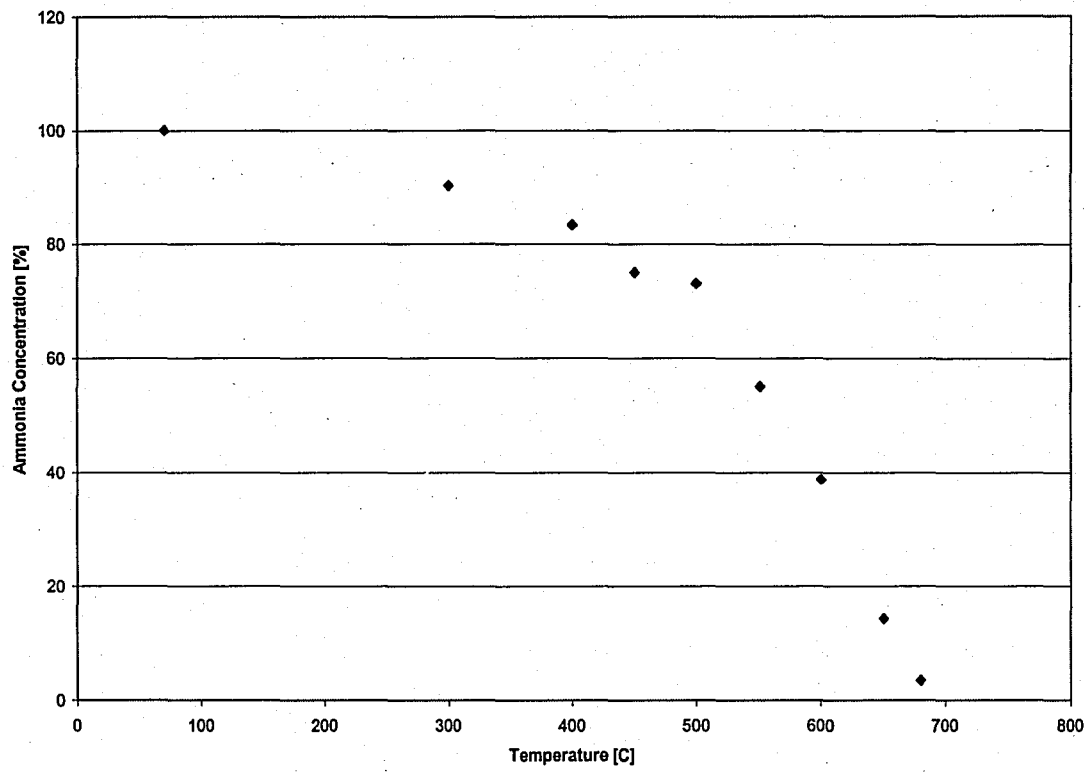

Figure 4.15: Ammonia Concentration as a Percent of the Original Concentration

Ammonia Removal in the Continuous Bed. The last set of experiments was designed to test the continuous removal of ammonia from the contaminated ash. These tests were designed to evaluate how well the bed removes ammonia from the ash at different flow rates. To perform this test, all fly ash from previous tests was removed from the bed. Next, the fluidizing air, speakers, and screw feeder were turned on and the heated section was filled with the ammonia contaminated ash. This section was observed for fluidization characteristics. To achieve good fluidization the air velocity was increased to 3.39 cm/s. The heaters were turned on and the ash was heated to 399 C. Next, the screw feeder was turned on at a speed of 10 rpm. This test was carried out for one hour. Temperature and flow rate measurements were taken every five minutes.

The flow rate samples were taken from the ash discharged from the bed. Ash did not begin to exit the bed until 30 minutes after the test began because the cooled section was empty when the test started. The ash used to measure the flow rate was divided into two samples. One sample was placed in a glass jar for an ammonia content testing and the rest of the sample was placed in a plastic bag for LOI testing. Sample time and number were recorded for both samples. Samples were also taken from the ash just before it entered the screw feeder to monitor the input ammonia concentration and LOI. The ammonia concentration and LOI of the samples were determined using the same procedures as described previously in this chapter. The screw feeder was increased to 15 rpm for 1 hour and then 20 rpm for 1 hour.

As shown in previous tests, the peak temperature of the ash decreased as the mass flow rate was increased. Figure 4.16 shows the peak temperature and the mass flow rate as a function of time.

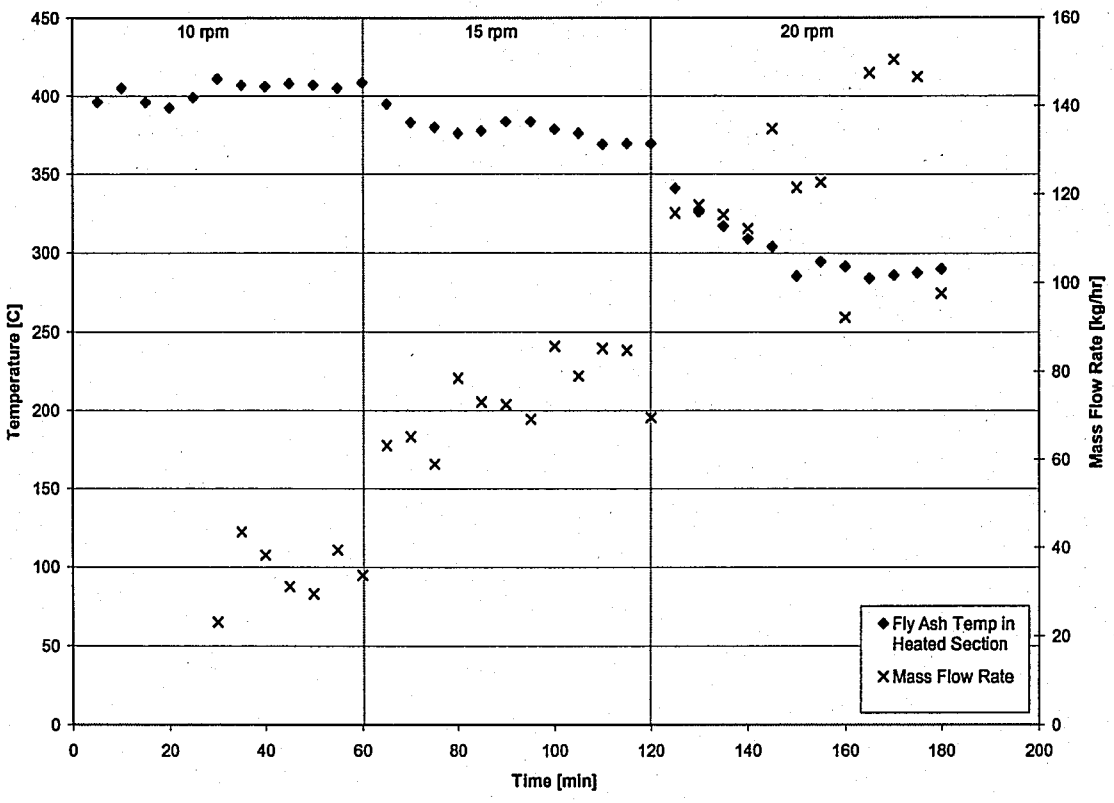

Figure 4.16: Peak Fly Ash Temperature and Mass Flow Rate for the Entire Test

Figure 4.17 shows the ammonia concentration of the output ash and temperature as a function of time. The ammonia removal was successful until the screw feeder speed was increased to 20 rpm.

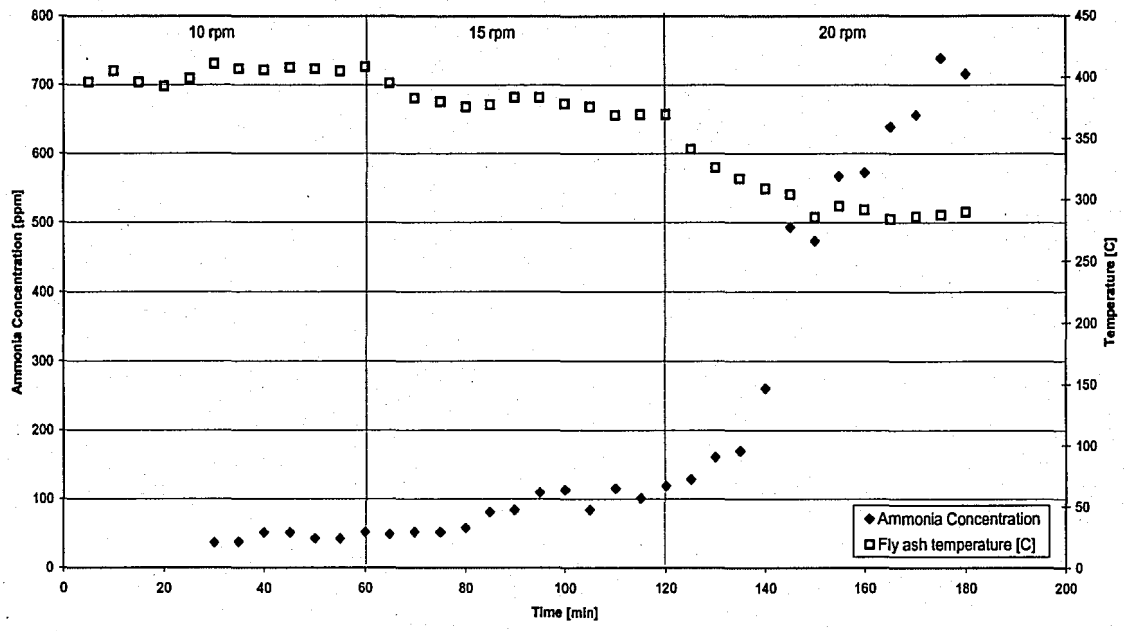

Figure 4.17: Ammonia Concentration and Ash Temperature for the Entire Test

Figure 4.18 shows the mass flow rate and the ammonia concentration. The ammonia concentration was reduced sufficiently for mass flow rates less than 80 kg/hr. Higher flow rates yielded unacceptable levels of ammonia still present in the fly ash.

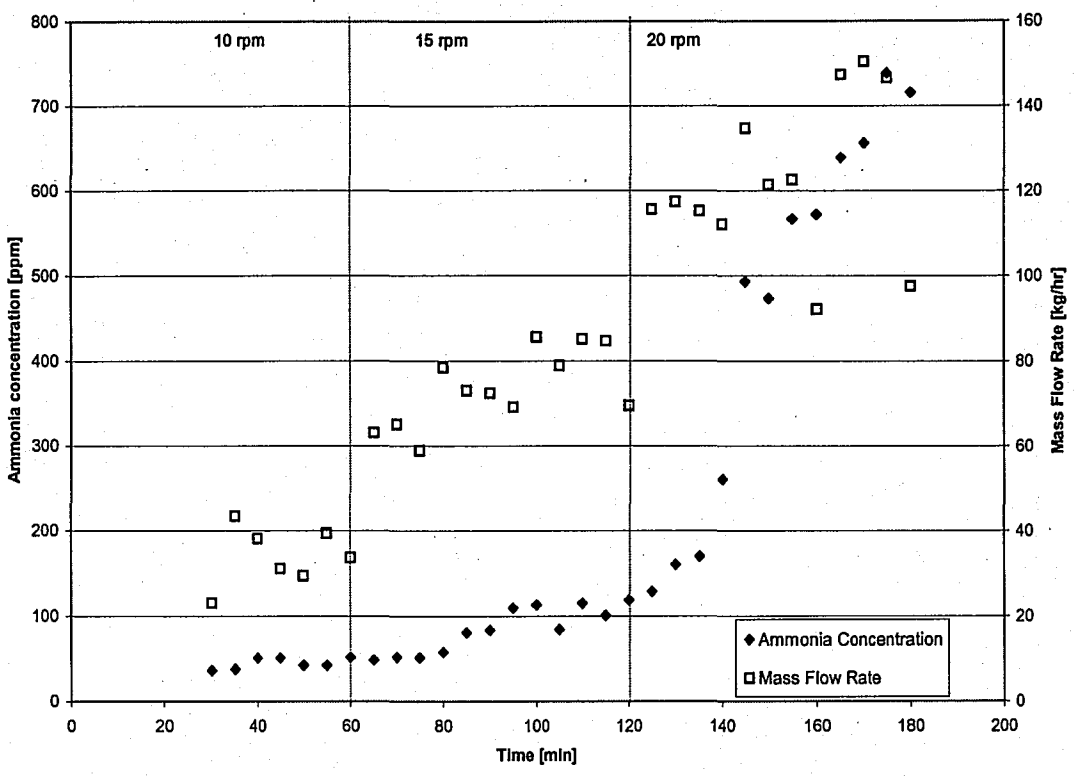

Figure 4.18: Ammonia Concentration and Mass Flow Rate for the Entire Test

To ensure that the continuously operating bed was operating properly, the results from this test were compared to the ammonia removal in the batch bed. To do this the ammonia concentrations were divided by the input concentration (1151 ppm) to obtain the ammonia concentration as a percent. The ammonia concentrations of both the continuously operating bed and the batch bed tests were then plotted against the ash temperature. Figure 4.19 shows the results. This figure shows that the results from both tests were similar and that the continuously operating bed was operating as expected.

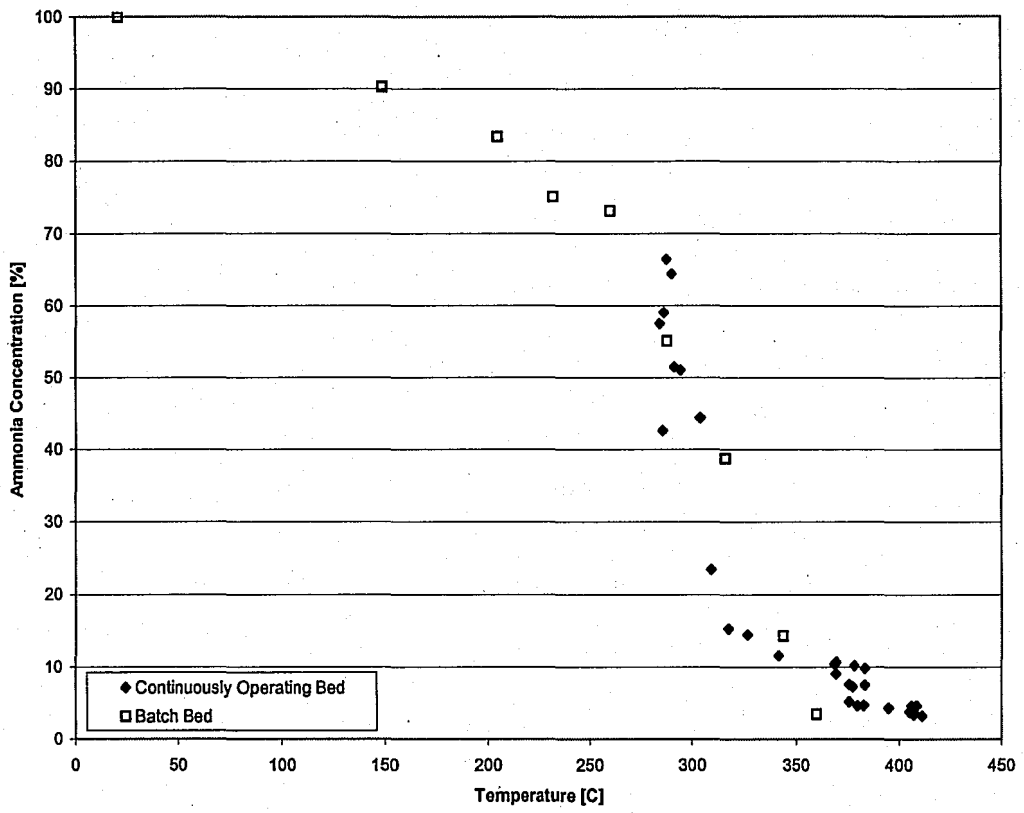

Figure 4.19: Ammonia Concentrations for Tests in the Batch Bed and the Continuously Operating Bed

Processing the ash through the continuously operating bed was expected to have little or no effect on the LOI of the ash. To remove the LOI, the ash must reach higher temperatures for longer periods of time. The ash that entered the bed had an LOI of 12.56 %. According to the results, the LOI of the ash increased. One possible explanation for the increased LOI is that some of the fines were removed during processing. The fine particles of the ash contain very small amounts of LOI. During the operation, some of the ash exited the bed through the joints in the bed and through the filtration system. To prove that this loss of ash contributed to the LOI results the particle size distribution of the output ash was checked at all three flow rates. As expected the output ash had a

higher mean particle size. This larger particle size accounts for the increased value of LOI. Figure 4.20 shows the LOI and the mean particle size.

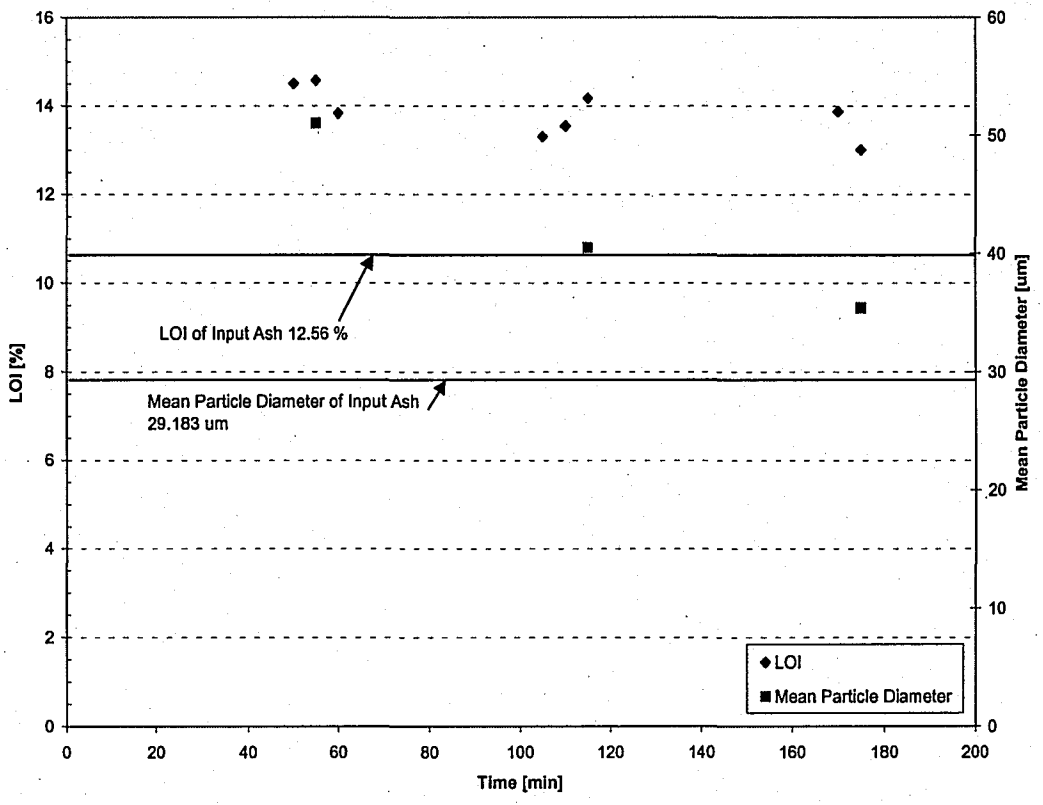

Figure 4.20: LOI and Mean Particle Size of the Processed Ash

CHAPTER 5: ENERGY BALANCE

To determine the cause of the lower than expected maximum mass flow rate of ash, an energy balance was performed on the system. The energy balance of the system is governed by equation 5.1.

$$q_{heaters} = \dot{m}_{ash}\dot{c}_{ash}\Delta T + \dot{m}_{air}c_{air}\Delta T + q_{sidewalls} \tag{5.1}$$

where $q_{heaters}$ is the total power dissipated by the heaters and $q_{sidewalls}$ is the heat lost from the side walls due to forced convection and radiation. The calculations were based on the conditions of the system at ash feeder speeds of 15 and 20 rpm during the ammonia removal test in the continuous bed.

Screw Feeder Calibration

Before any calculations were carried out, the screw feeder was calibrated to ensure that the flow rate measurements taken at the exit of the bed were consistent with rate of ash input into the bed. These measurements were performed by weighing a timed sample of ash deposited into the bed by the screw feeder. Table 5.1 shows the results. These results are consistent with the values measured at the exit end of the bed.

10 rpm	45.36 kg/hr
15 rpm	77.11 kg/hr
20 rpm	122.47 kg/hr

Table 5.1: Calibration of the Screw Feeder

Heat Loss Calculations

To calculate the heat lost from the side walls, first the temperature of the side walls had to be estimated since no data was taken on sidewall temperature. To estimate the sidewall temperature, the radiation effects were considered. The wall was split into three sections each with a height of 0.3 m. To find the surface temperature of each section the radiation from the free surface of the fly ash to the side walls was set equal to the radiation from the side wall to the surroundings. The radiation was assumed to be black body radiation. Figure 5.1 shows the problem diagram. A_1 is the entire surface area of the fly ash and A_2, A_3, and A_4 are the areas of the 3 sections of side wall (0.3 x 1.8288 m).

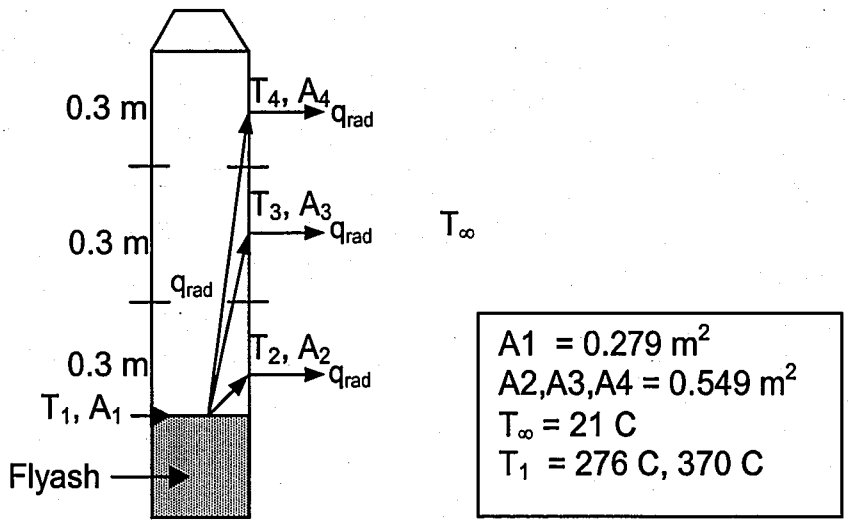

Figure 5.1: Diagram for Radiation Calculations

Equation 5.2 was used to calculate T_n.

$$A_1 F_{1,n} \sigma (T_1^4 - T_n^4) = A_n \sigma (T_n^4 - T_\infty^4) \tag{5.2}$$

where $F_{1,n}$ is the shape factor, σ is the Stefan-Boltzman constant, and n varies from 2 to 4. Figure 5.2 shows the results of this calculation. The side wall temperatures are underestimated since internal free convection and conduction were not considered.

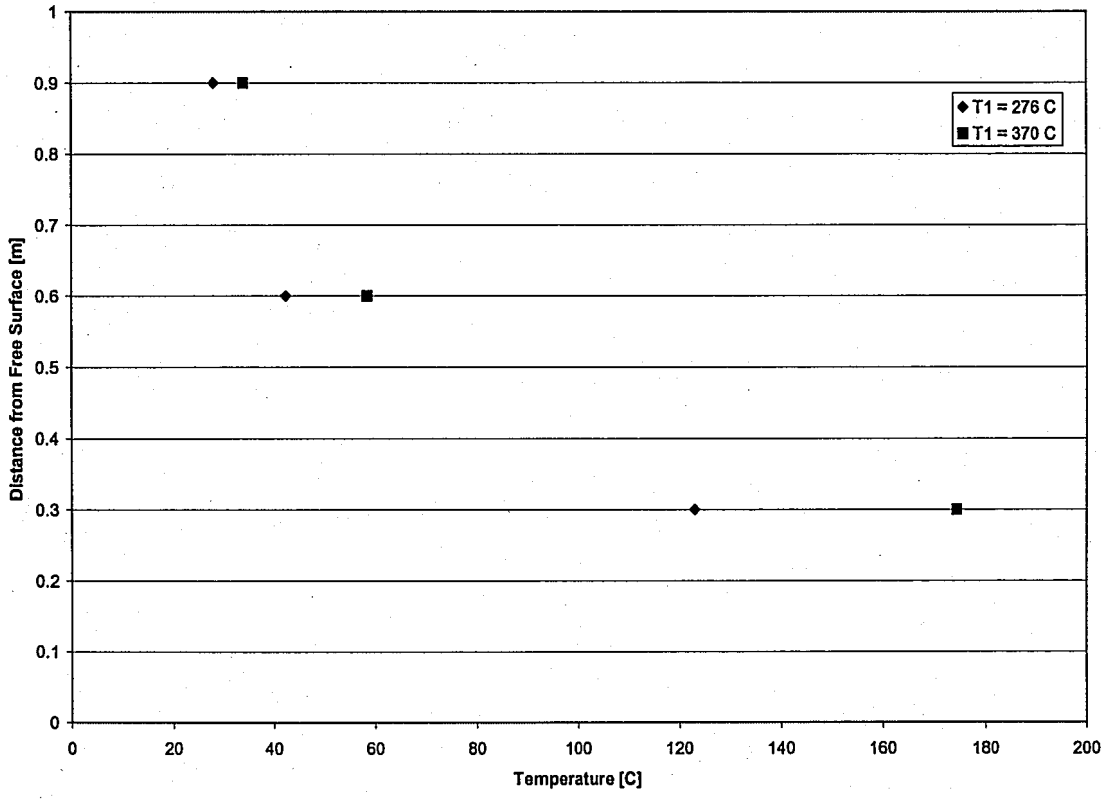

Figure 5.2: Calculated Sidewall Temperature Distributions

The calculated side wall temperatures were then used to calculate the heat lost from the side walls by free convection and radiation. The governing equation for convection is

$$q_{conv} = \sum_{n=2}^{4} 2\bar{h}_n A_n (T_n - T_\infty) \tag{5.3}$$

where $\bar{h}_n$ is the average heat transfer coefficient, A_n is the area of the wall, T_n is the wall temperature and T_∞ is the air temperature. The factor of 2 is used to account for both side walls. To solve this equation the Rayleigh number was calculated by Equation 5.4

$$Ra_L = \frac{L^3 g\beta(T_n - T_\infty)}{\alpha v} \tag{5.4}$$

where g is the gravitational acceleration, β is $1/T_f$, α is the thermal diffusivity, and v is the viscosity. Then the Nusselt number was calculated by[8]

$$\overline{Nu}_L = \left\{ 0.825 + \frac{0.387 Ra_L^{1/6}}{\left[1 + (0.492/\Pr)^{9/16}\right]^{4/9}} \right\} \tag{5.5}$$

The heat transfer coefficient was then found by solving Equation 5.6.

$$\bar{h}_n = \frac{\overline{Nu}_L k}{L} \tag{5.6}$$

where k is the thermal conductivity.

The radiation losses were then calculated by Equation 5.7.

$$q_{rad} = \sum_{n=2}^{4} 2 A_n \sigma (T_n^4 - T_\infty^4) \tag{5.7}$$

The factor of 2 in equation 5.7 is included because there are two side walls.

Conditions and Assumptions		
Ash Feeder Speed	15 rpm	20 rpm
A_1	0.279 m^2	0.279 m^2
A_2, A_3, A_4	0.549 m^2	0.549 m^2
L	0.3 m	0.3 m
$\dot{m}_{ash}$	0.02167 kg/s	0.03402 kg/s
$\dot{m}_{air}$	0.0109624 kg/s	0.0109624 kg/s
T_1	370 C	276 C
T_∞	21 C	21 C
T_{air} (internal)	370 C	276 C

Table 5.2: Summary of Conditions and Assumptions Made in the Energy Balance

Table 5.3 shows the results of the calculations. The heat lost due to convection radiation at 15 rpm is greater than the heat lost at 20 rpm because the temperature of the fly ash was higher.

The heater resistance was measured at operating temperature and was approximately 7% higher than at room temperature. Therefore, the actual output of the heaters was less at operating temperature than it would be at room temperature. The total power of the heaters was calculated by

$$q_{heaters} = \frac{nV_{rms}^2}{R} \tag{5.8}$$

where n is the number of heaters, V_{rms} is the RMS voltage and R is the resistance. The heat gained by the fluidization air, q_{air} is larger at an ash feeder speed of 15 rpm because the ash temperature is higher. The air temperature as it leaves the surface temperature of the ash is assumed to be equal to the ash temperature. The energy balance accounts for 89 percent of the input power for 15 rpm and 81 percent of the input power for 20 rpm. The remaining heat losses can be accounted for in the underestimation of the sidewall temperature and radiation and convection losses from the plate to which the speakers are mounted and the plenum.

Results		
Ash Feeder Speed	15 rpm	20 rpm
q_{air}	3841.62 W	2925.37 W
q_{ash}	6962 W	8312 W
$q_{freeconv}$	1650.75 W	939.68 W
q_{rad}	2398.25 W	1260.86 W
q_{total}	14852.62 W	13437.91 W
q_{heater}	16621 W	16621 W
q_{heater}-q_{total}	1768 W	3183 W

Table 5.3: Summary of the Results of the Energy Balance

CHAPTER 6: CONCLUSIONS AND RECOMMENDATIONS

Conclusions

A continuously operating fluidized bed has been designed, built, and tested for the removal of ammonia from fly ash. Based on the results of this study, it can be concluded that

1. A continuously operating fluidized bed is an effective way to remove ammonia from fly ash; 95 percent of initial ammonia concentration can be removed during continuous operation above 385 C.
2. Good fluidization and bubbling were achieved in the new bed after some modifications were made to the air distribution system;
3. Tests performed with the continuously operating bed display similar trends and ammonia removal results to those tests performed with the batch bed;
4. Energy losses to the fluidization air and from the side walls led to an operating mass flow rate of ash less than the fluidized bed was designed for.

Recommendations

In order to process larger mass flow rates of ash the heat losses from the

system must be minimized. The best way to minimize the heat losses is to insulate the side walls. Then the heater power would only need to be increased to overcome the losses consumed by the fluidizing air.

To monitor the heaters and to ensure that they are operating properly two digital ammeters should be installed for each contactor box. Each contactor box is connected to two separate banks of heaters, one on each side of the bed, with an equal number of heaters. The ammeters should be connected so that the current to each bank can be monitored. If one or more heaters are not functioning there will be a discrepancy between the readings on the two ammeters. Analog ammeters should not be used because each heater uses approximate 1.3 A. This difference would be difficult to deduce from an analog ammeter.

Testing should be continued in the laboratory with contaminated fly ashes from other power plants to ensure that the system is capable of handling them. The system should then be setup and tested at a coal burning facility with the input ash coming directly from a silo.

REFERENCES

[1] World Coal Institute. Http://www.wci-coal.com/facts_coal99.htm.

[2] B.E. Scheetz and R. Earle, Utilization of fly ash, *Current Opinion in Solid State and Materials Science, Volume 3, Issue 5, October 1998, Pages 510-520.*

[3] F.W. van der Brugghen, J.W. van dn Berg, W.H. Kuiper, and R. Visser, Problems Encountered During the use of Ammonium-Contaminated Fly Ash, *EPRI/EPA Joint Symposium on Stationary Combustion NO_x Control, 1995.*

[4] D. Huang, unpublished results.

[5] L. Leu, J. Li, C. Chen, Fluidization of Group B Particles in an Acoustic Field, *Powder Technology, Volume 94, Issue 1, November 1997, Pages 23-8.*

[6] C. Herrera, Acoustic Characteristics of Fine Powders in Fluidized Beds, PhD Dissertation, Lehigh University, May 2000.

[7] Instruction Manual for Fisher Scientific Ammonia Ion Selective Electrode, Catalog No. 13-620-504.

[8] F.P. Incropera, and D.P.DeWitt, *Fundamentals of Heat and Mass Transfer, John Wiley & Sons, Inc. 1996*, Pages 360, 494-495.

VITA

Kenneth Bradford Lawton was born in Bristol, Pennsylvania on February 14, 1978 to Kenneth and Sheran Lawton. He graduated from Mansfield Jr./Sr. High School in 1996. He continued his education at Mansfield University, graduating in December 19, 1999 with a Bachelor of Science Degree in Physics. He started his graduate study in Mechanical Engineering at the University of Pittsburgh in January 2000. After one semester he transferred to Lehigh University, obtaining his Masters of Science Degree in Mechanical Engineering in June, 2002.

END OF

TITLE